Nonstandard Yukawa Couplings and Higgs Portal Dark Matter

Fady Bishara,[1, 2, *] Joachim Brod,[3, †] Patipan Uttarayat,[4, ‡] and Jure Zupan[1, §]

[1]*Department of Physics, University of Cincinnati, Cincinnati, Ohio 45221,USA*

[2]*Theoretical Physics Department, Fermilab, P.O. Box 500, Batavia, IL 60510*

[3]*PRISMA Cluster of Excellence & Mainz Institute for Theoretical*

Physics, Johannes Gutenberg University, 55099 Mainz, Germany

[4]*Department of Physics, Srinakharinwirot University,Wattana, Bangkok 10110 Thailand*

Abstract

We study the implications of non-standard Higgs Yukawa couplings to light quarks on Higgs-portal dark matter phenomenology. Saturating the present experimental bounds on up-quark, down-quark, or strange-quark Yukawa couplings, the predicted direct dark matter detection scattering rate can increase by up to four orders of magnitude. The effect on the dark matter annihilation cross section, on the other hand, is subleading unless the dark matter is very light – a scenario that is already excluded by measurements of the Higgs invisible decay width. We investigate the expected size of corrections in multi-Higgs-doublet models with natural flavor conservation, the type-II two-Higgs-doublet model, the Giudice-Lebedev model of light quark masses, minimal flavor violation new physics models, Randall-Sundrum, and composite Higgs models. We find that an enhancement in the dark matter scattering rate of an order of magnitude is possible. Finally, we point out that a discovery of Higgs-portal dark matter could lead to interesting bounds on the light-quark Yukawa couplings.

---

[*]Electronic address:fadybishara@gmail.com

[†]Electronic address:joachim.brod@uni-mainz.de

[‡]Electronic address:patipan@g.swu.ac.th

[§]Electronic address:zupanje@ucmail.uc.edu

I. INTRODUCTION

In Higgs-portal models [1–10] of dark matter (DM) the Higgs is usually assumed to be completely Standard Model (SM) like apart from its couplings to DM. Experimentally, only the couplings of the Higgs to the heaviest particles of the SM are currently well constrained. The couplings to gauge bosons are found to be in agreement with the SM predictions at the $\mathcal{O}(20\%)$ level, while the constraints on the couplings to third-generation fermions are somewhat weaker [11, 12]. Much less is known experimentally about the couplings of the Higgs to the first two generations of fermions. The couplings to u, d, s, and c quarks could be as large as the SM bottom Yukawa coupling or be absent altogether [13–16]. The Higgs couplings to top and bottom quarks will be quite well known by the end of the high-luminosity LHC run. Some progress is also expected on the measurements of Higgs couplings to charm and strange quarks [13–15].

Large u-, d-, and s-quark Yukawa couplings, comparable in size to the b-quark Yukawa, generically require fine-tuning. A large Yukawa coupling implies a large contribution to the quark mass from the Higgs vacuum expectation value (vev). This would then need to be cancelled by a different contribution to the u-, d-, and s-quark masses, unrelated to the Higgs vev. The opposite limit, where the observed Higgs does not couple to the light quarks at all is easier to entertain. It simply requires a separate source of the light-quark masses (for an extreme example see, e.g., [17]).

Modified light-quark Yukawa couplings could, in principle, have important implications for DM phenomenology. In this article we investigate how the Higgs-portal DM predictions change if the Higgs couplings to the light quarks differ from the SM expectations. We first allow for an arbitrary flavor structure of the Higgs Yukawa couplings, only requiring that they satisfy the current experimental bounds. In Section II we derive the implications for direct DM detection, indirect DM detection and the collider searches. We show that vanishing couplings of the Higgs to light quarks only have a relatively small impact on these observables. Saturating the loose current bounds on the light-quark Yukawa couplings would, on the other hand, lead to drastically enhanced scattering cross sections on nuclei while leaving the relic density and annihilation cross sections nearly unmodified.

Clearly, an enhancement of the light-quark Yukawas by factors of $\mathcal{O}(100)$ or more, as allowed by current data, requires considerable fine tuning of the quark-mass terms and

hence seems quite unlikely. In Section III we, therefore, explore the deviations in the Higgs Yukawa couplings for a number of beyond-the-SM scenarios and flavor models. This leads to more realistic expectations as to how large the deviations in the direct DM detection rates can be due to the poorly known Higgs couplings to the light quarks. Note that we assume the DM to be a flavor singlet and that the new flavor structure of the interactions with the visible sector is only due to the modification of the SM Higgs couplings. DM that is in a nontrivial flavor multiplet has been investigated in [18–29], while our study is closer in spirit to the work in [30–32] where the flavor dependence of the DM signals for flavor-singlet DM has been explored.

A somewhat surprising result of our investigation is that, if DM is discovered and turns out to be a thermal relic predominantly interacting through a Higgs portal, it could be used to constrain the light-quark Yukawa couplings. This is discussed in more detail in Section IV.

We summarize our results in Section V.

II.   HIGGS PORTAL WITH NON-TRIVIAL FLAVOR STRUCTURE

We assume that DM and the SM fields are the only light degrees of freedom. The remaining new physics (NP) particles can be integrated out so that one can use an Effective Field Theory (EFT) approach. The couplings of DM to the SM are given by the Higgs-portal Lagrangian

$$\mathcal{L}_\chi = \begin{cases} g_\chi \chi^\dagger \chi H^\dagger H\,, & \text{scalar DM;} \\ g_\chi \dfrac{1}{\Lambda} \bar{\chi}\chi H^\dagger H + i\tilde{g}_\chi \dfrac{1}{\Lambda} \bar{\chi}\gamma_5\chi H^\dagger H\,, & \text{fermion DM;} \\ \dfrac{g_\chi}{2} \chi^\mu \chi_\mu H^\dagger H, & \text{vector DM.} \end{cases} \tag{1}$$

Above, the fermion DM can be either a Dirac or Majorana fermion (in either case we use four component notation). After electroweak symmetry breaking (EWSB) we have

$$H^\dagger H = \frac{1}{2}\big(v_W^2 + 2v_W h + h^2\big), \tag{2}$$

where $v_W = 246$ GeV is the vacuum expectation value (vev) of the Higgs field. The above interactions therefore lead to annihilation of DM into both single Higgs, $\chi\bar{\chi} \to h$, and double Higgs, $\chi\bar{\chi} \to hh$, final states.

The Higgs-portal operator for fermionic DM has mass dimension five and is suppressed by the new physics scale Λ. The Higgs-portal interaction for fermionic DM can also be

re-written as $\mathcal{L}_\chi = (g_\chi + i\tilde{g}_\chi)\bar{\chi}_L\chi_R H^\dagger H/\Lambda + \text{h.c.}$. For $\tilde{g}_\chi \neq 0$ the interaction is thus both P- and CP-violating. The interaction for vector DM is most probably also due to a higher-dimensional operator in the full theory. For instance, if χ_μ arises from a spontaneously broken gauge symmetry in the dark sector, then $g_\chi \sim v_D^2/\Lambda^2$, where v_D is the vev of the field that breaks the dark sector gauge invariance, while Λ is the mass of the mediator between DM and the Higgs.

The relevant terms, after EWSB, in the effective Lagrangian for the Higgs couplings to the SM particles are given by

$$\mathcal{L}_{\text{eff}} = -\kappa_q \frac{m_q}{v_W}\bar{q}qh - \kappa_\ell \frac{m_\ell}{v_W}\bar{\ell}\ell h + \kappa_V \left(\frac{2m_W^2}{v_W}W^{+\mu}W_\mu^- + \frac{m_Z^2}{v_W}Z^\mu Z_\mu\right)h$$
$$- \kappa_\lambda \frac{m_h^2}{2v_W}h^3 + \kappa_g^{\text{NP}} \frac{\alpha_s}{12\pi v_W}hG_{\mu\nu}^a G^{a\mu\nu} \tag{3}$$

where the κ_i are real. A sum over the SM quarks, $q = u, d, s, c, b, t$, and charged leptons, $\ell = e, \mu, \tau$ is implied, and we have assumed custodial symmetry. The $h \to \gamma\gamma$ coupling is not relevant for DM phenomenology, since its effects are suppressed compared to the Higgs couplings to gluons.[1] The couplings are normalized such that $\kappa_q = \kappa_\ell = \kappa_V = \kappa_\lambda = 1$ correspond to the SM. The experimental constraints on the couplings of the light quarks to the Higgs, obtained from a global fit to current data, are $|\kappa_u| < 0.98m_b/m_u$, $|\kappa_d| < 0.93m_b/m_d$, $|\kappa_s| < 0.70m_b/m_d$, where only one of the light Yukawa couplings was left to float in the fit, while all the other Higgs couplings are set to the SM values [13]. Higgs couplings to the light quarks of a size comparable to the coupling to the b quark are thus still allowed. In (3) we do not allow for flavor violating Higgs couplings, since these are already tightly constrained from both Higgs decays and low-energy observables [33–36].

In the SM, keeping the Higgs on shell, the hGG coupling arises predominantly from the one-loop top-quark contribution. The κ_g^{NP} in (3) encodes only the potential NP contributions, and vanishes in the SM. In the global fits a parameter κ_g is introduced that gives the total $h \to gg$ amplitude, including the SM contributions [11, 12]. We have (see, e.g., [37])

$$\kappa_g \simeq 1.03\kappa_t + \kappa_g^{\text{NP}}. \tag{4}$$

---

[1] It could be relevant for direct detection if the scattering on electrons dominates. This requires very light DM, of order the electron mass. Such light Higgs-portal DM is excluded by the constraints on the Higgs invisible branching ratio.
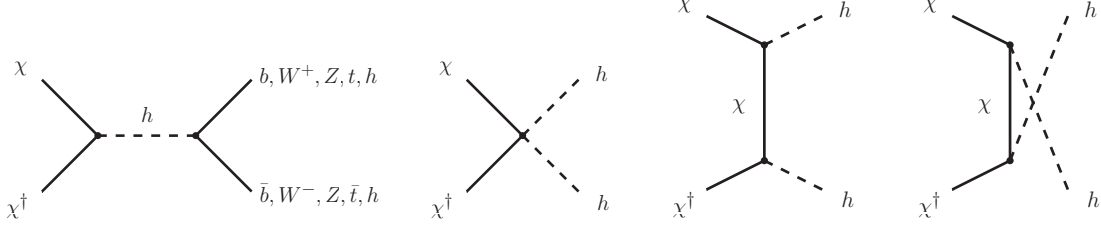
Figure 1: DM annihilation channels in the Higgs-portal models.

At present, significant CP-violating Higgs couplings to fermions and gluons are still allowed experimentally (see, e.g., [38]), so we also discuss their effect on the Higgs interactions with DM:

$$\mathcal{L}_{\text{eff,CPV}} = -i\tilde{\kappa}_q \frac{m_q}{v_W} \bar{q}\gamma_5 q h - i\tilde{\kappa}_\ell \frac{m_\ell}{v_W} \bar{\ell}\gamma_5 \ell h + \tilde{\kappa}_g^{\text{NP}} \frac{\alpha_s}{8\pi v_W} h G_{\mu\nu}^a \widetilde{G}^{a\mu\nu} . \tag{5}$$

Here, the $\tilde{\kappa}_i$ are real parameters; in the SM, we have $\tilde{\kappa}_i = 0$. Moreover, $G_{\mu\nu}^a$ is the gluon field-strength tensor and $\widetilde{G}^{a,\mu\nu} = \frac{1}{2}\epsilon^{\mu\nu\alpha\beta} G_{\alpha\beta}^a$ its dual. The normalization of the $hG\tilde{G}$ term is chosen such that integrating out the top at one loop one obtains $\tilde{\kappa}_g = \tilde{\kappa}_t + \tilde{\kappa}_g^{NP}$. Accordingly, we have $\text{Br}(h \to gg) \propto \kappa_g^2 + (3\tilde{\kappa}_g/2)^2$. The CP-violating couplings of the Higgs to ZZ and WW are already well constrained, and we thus set them to zero. In the numerical analysis below, we will also assume $\tilde{\kappa}_i = 0$, for simplicity.

The modified Higgs couplings change the usual Higgs-portal predictions for DM annihilation rates, the relic abundance, and direct detection rates. In the following, we discuss these modifications in detail.

A. Annihilation cross sections

The dominant DM annihilation cross sections in the Higgs-portal models are $\chi\bar{\chi} \to b\bar{b}, W^+W^-, ZZ, t\bar{t}$, and $\chi\bar{\chi} \to hh$. The first four proceed through the s-channel Higgs exchange, while $\chi\bar{\chi} \to hh$ receives additional contributions from t- and u-channel χ exchange as well as from the four-point contact interaction (cf. Fig. 1). The $\chi\bar{\chi} \to b\bar{b}$ channel is only relevant if the other channels are not kinematically allowed, i.e. for light DM masses, $m_\chi < m_W$.

The $\chi\bar{\chi} \to \bar{b}b$ annihilation cross section assuming SM Higgs couplings is given for scalar

(S), Dirac fermion (DF), and vector (V) DM by

$$\left(\sigma_{b\bar{b}}^{S} v_{\mathrm{rel}}\right)_{SM} = \frac{N_c}{4\pi} \frac{g_\chi^2 m_b^2 \beta_b^3}{(s - m_h^2)^2 + m_h^2 \Gamma_h^2} \, , \tag{6}$$

$$\left(\sigma_{b\bar{b}}^{DF} v_{\mathrm{rel}}\right)_{SM} = \frac{N_c}{8\pi} \frac{m_b^2}{\Lambda^2} \frac{g_\chi^2 \left(s - 4m_\chi^2\right) + \tilde{g}_\chi^2 s}{(s - m_h^2)^2 + m_h^2 \Gamma_h^2} \beta_b^3 \, , \tag{7}$$

$$\left(\sigma_{b\bar{b}}^{V} v_{\mathrm{rel}}\right)_{SM} = \frac{N_c}{9} \frac{g_\chi^2}{16\pi} \frac{m_b^2}{m_\chi^4} \beta_b^3 \left(1 - r_\chi + \frac{3}{4}r_\chi^2\right) \frac{s^2}{(s - m_h^2)^2 + m_h^2 \Gamma_h^2} \, , \tag{8}$$

where, here and below, $\sqrt{s}$ is the center-of-mass energy, $r_k = 4m_k^2/s$, $\beta_k = \sqrt{1 - r_k}$ is the velocity of particle k, and $v_{\mathrm{rel}} = 2\beta_\chi$ is the relative velocity of the DM particles. If the Higgs coupling to the b-quarks differs from the SM value, the annihilation cross section is rescaled as

$$\sigma_{b\bar{b}} = \left(\kappa_b^2 + \tilde{\kappa}_b^2/\beta_b^2\right)\sigma_{b\bar{b}}^{\mathrm{SM}} \, . \tag{9}$$

The annihilation cross sections $\sigma_{f\bar{f}}$ to the other fermions are obtained with the obvious replacement $b \to f$ in the above expressions. Since the Higgs couplings to the light quarks are poorly constrained experimentally, the DM annihilation to two light quarks can be comparable to $\chi\bar{\chi} \to b\bar{b}$ and can be important for light DM, $m_\chi < m_W$.

For heavy DM, $m_\chi > m_W$, the annihilation cross-sections into a pair of W or Z bosons are

$$\sigma_{VV} = \kappa_V^2 \sigma_{VV}^{\mathrm{SM}} \, , \tag{10}$$

$V = W, Z$. The annihilation cross sections assuming the SM Higgs couplings to W are given by

$$(\sigma_{WW}^{S} v_{\mathrm{rel}})_{\mathrm{SM}} = \frac{g_\chi^2}{8\pi} \beta_W \left(1 - r_W + \frac{3}{4}r_W^2\right) \frac{s}{(s - m_h^2)^2 + m_h^2 \Gamma_h^2} \, , \tag{11}$$

$$(\sigma_{WW}^{DF} v_{\mathrm{rel}})_{\mathrm{SM}} = \frac{1}{16\pi\Lambda^2} \beta_W \left(1 - r_W + \frac{3}{4}r_W^2\right) \frac{s \left[g_\chi^2 \left(s - 4m_\chi^2\right) + \tilde{g}_\chi^2 s\right]}{(s - m_h^2)^2 + m_h^2 \Gamma_h^2} \, , \tag{12}$$

$$(\sigma_{WW}^{V} v_{\mathrm{rel}})_{\mathrm{SM}} = \frac{g_\chi^2}{288\pi} \frac{s}{m_\chi^4} \beta_W \left(1 - r_W + \frac{3}{4}r_W^2\right) \left(1 - r_\chi + \frac{3}{4}r_\chi^2\right) \frac{s^2}{(s - m_h^2)^2 + m_h^2 \Gamma_h^2} \, , \tag{13}$$

for scalar, Dirac fermion, and vector DM, respectively. The $\chi\bar{\chi} \to ZZ$ annihilation cross section is obtained by replacing $W \to Z$, and multiplying all expressions by an extra factor of $1/2$ since one has two indistinguishable particles in the final state.

The $\chi\bar{\chi} \to hh$ annihilation cross sections for scalar, Dirac fermion, and vector DM, are

given by

$$\sigma_{hh}^{S} v_{\rm rel} = \frac{\beta_h g_\chi^2}{64\pi m_\chi^2} \left[1 + \frac{3\kappa_\lambda M_h^2}{4m_\chi^2 - M_h^2} - \frac{2v_W^2 g_\chi}{M_h^2 - 2m_\chi^2} \right]^2, \tag{14}$$

$$\sigma_{hh}^{DF} v_{\rm rel} = \frac{\beta_h (\tilde{g}_\chi^2 + g_\chi^2 \beta_\chi^2)}{32\pi \Lambda^2} \left[1 + \frac{3\kappa_\lambda M_h^2}{4m_\chi^2 - M_h^2} + \frac{4g_\chi m_\chi v_W^2}{\Lambda(2m_\chi^2 - M_h^2)} \right]^2, \tag{15}$$

$$\sigma_{hh}^{V} v_{\rm rel} = \frac{\beta_h}{576\pi m_\chi^2} \left[3g_\chi^2 \left(\frac{3\kappa_\lambda M_h^2}{4m_\chi^2 - M_h^2} + 1 \right)^2 + \frac{4g_\chi^4 v_W^4}{(2m_\chi^2 - M_h^2)^2} \left(6 - \frac{4M_h^2}{m_\chi^2} + \frac{M_h^4}{m_\chi^4} \right) \right.$$

$$\left. + \frac{16g_\chi^3 v_W^2}{2m_\chi^2 - M_h^2} \left(\frac{3\kappa_\lambda M_h^2}{4m_\chi^2 - M_h^2} + 1 \right) \left(1 - \frac{M_h^2}{4m_\chi^2} \right) \right]. \tag{16}$$

In this result we display only the leading terms in the expansion in powers of β_χ. The contribution of the s-channel Higgs exchange diagram is proportional to the rescaling of the trilinear Higgs coupling, κ_λ. The latter is completely unknown experimentally, at present, but can be measured to $\mathcal{O}(20\%)$ at the end of the LHC [39, 40]. Since we are mostly interested in the effects of flavor modifications we will set it to the SM value, $\kappa_\lambda = 1$, in the numerics below. All cross sections for Majorana DM can be obtained by multiplying the corresponding Dirac DM cross sections by a factor of 4.

B. Relic abundance

The DM relic abundance Ω_{DM} is proportional to $1/\sigma v_{\rm rel}$, where σ is the annihilation cross section. Assuming that the DM in our scenario accounts for all of the observed relic density, the measured value $\Omega_{DM} h^2 = 0.1198(26)$ [41] fixes g_χ for a given value of m_χ. The resulting constraint in the $m_\chi - g_\chi$ plane is denoted for the different cases by a red line in Figs. 2 to 9. In Fig. 2, we compare two limits of the Higgs portal for the scalar DM: the case where the Higgs does not couple to the light quarks at all (left panel) to the case where the Higgs has SM Yukawa couplings (right panel). The two relic abundance curves coincide apart from very light DM, with m_χ below the charm and tau threshold. If such light DM did not couple to the u, d and s quarks, this would result in noticeably reduced annihilation cross sections and, thus, in larger relic abundance. In both cases, the dominant annihilation process is still given by $\chi\bar\chi \to h^* \to gg$. For very light DM the correct relic abundance is obtained only if the coupling of the Higgs to DM, g_χ, is nonperturbatively large. The yellow regions in Fig. 2 denote the value of g_χ for which the total Higgs decay width would be larger than
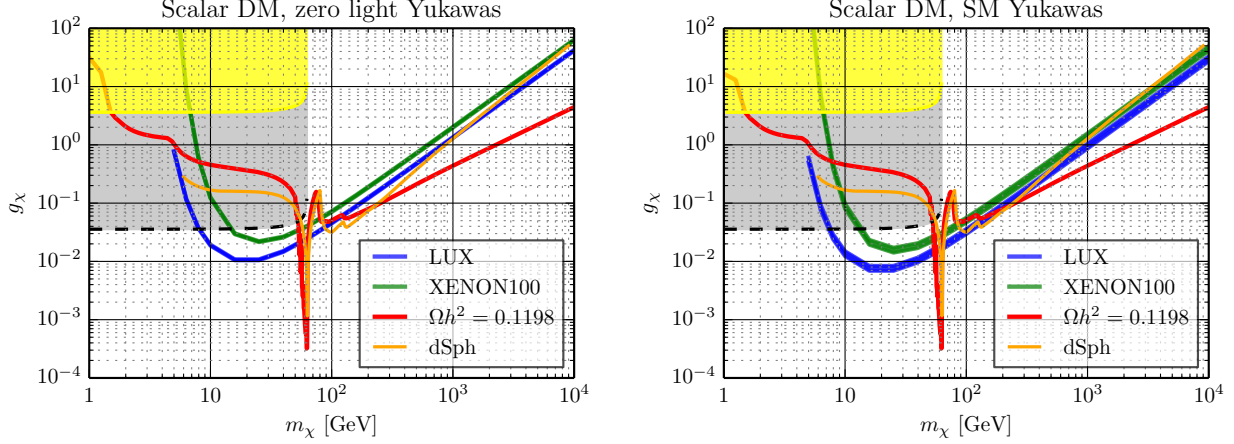
Figure 2: Bounds from LUX (blue band), XENON100 (green band) and the invisible Higgs decay width (black dashed line and grey region) on the Higgs-portal coupling g_χ for scalar DM, assuming vanishing (left) and SM (right) Yukawa couplings to u, d, s quarks. The red line denotes g_χ as a function of DM mass, m_χ, for which the correct relic abundance is obtained, while g_χ in the yellow region leads to non-perturbatively large Higgs decay width, $\Gamma_h > m_h$, and is excluded. Constraints from Fermi-LAT searches for DM annihilation in dwarf spheroidal galaxies are denoted by the orange band.

its mass, $\Gamma_h > m_h$, and are thus excluded.

The same comments apply to the case of vector DM, shown in Fig. 4, CP-conserving Dirac fermion DM, shown in Fig. 6, CP-violating Dirac fermion DM, shown in Fig. 8, and also for Majorana fermion DM. For light DM, $m_\chi \lesssim 30$ GeV, the correct relic density requires a non-perturbatively large coupling g_χ so that the predictions should be taken only as $\mathcal{O}(1)$ estimates in that region. Note that all these non-perturbative regions are, in addition, excluded by bounds on the decay width of the Higgs into invisible final states (see the discussion in Section II C).

In Figs. 3, 5, 7, and 9, we show the relic abundance curves for g_χ as a function of m_χ for the case where the light Yukawa couplings saturate their upper experimental bound. The left panels show the case where $\kappa_u = 0.98 m_b/m_u$ and all the other couplings at their SM values, the middle panels the case where $\kappa_d = 0.93 m_b/m_d$, and the right panels the case where $\kappa_s = 0.70 m_b/m_s$. In all of these cases the cross section for DM annihilation to light jets, $\sigma(\chi\bar{\chi} \to jj)$, coming from DM annihilating to light quarks, is comparable to the annihilation
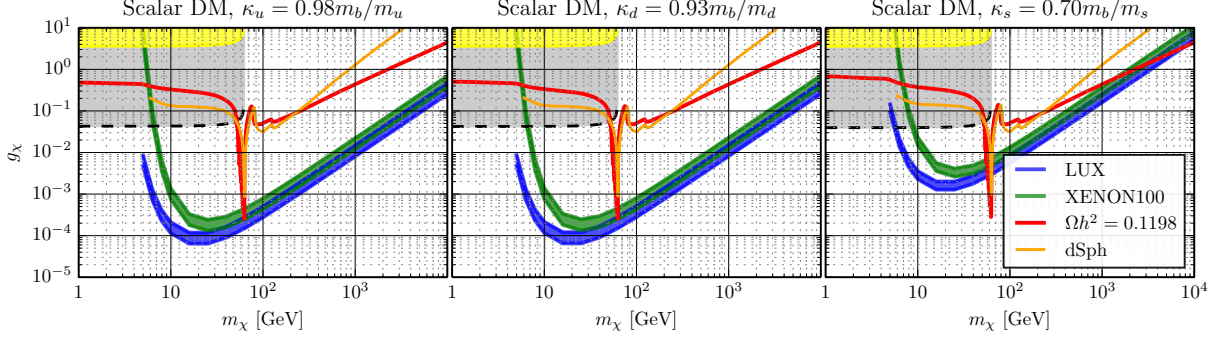
Figure 3: Bounds on the Higgs-portal coupling g_χ for scalar DM, assuming maximal allowed values for the Yukawa couplings to the u, d, s quarks (left to right), keeping all the other couplings to their SM values. The color coding is the same as in Fig. 2.
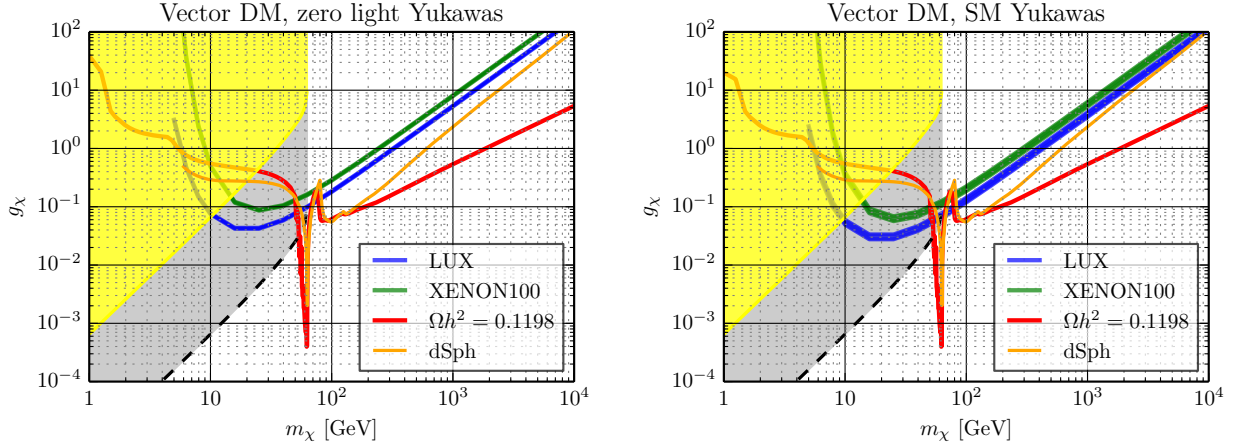

Figure 4: Bounds on the Higgs-portal coupling for vector DM, assuming vanishing (left) and SM (right) Yukawa couplings to u, d, s quarks. The color coding is the same as in Fig. 2.

cross section to b-jets, $\sigma(\chi\bar{\chi} \to b\bar{b})$. For $m_\chi \lesssim m_W$ these are the two dominant annihilation modes. Since the annihilation cross sections to b-jets and light jets are comparable, the relic abundance curve show only a small change in g_χ when the b-quark threshold is reached. This should be compared with the case of the SM Yukawa couplings shown in the right panels of Figs. 2, 4, 6, and 8. In this case the $\chi\bar{\chi} \to jj$ annihilation is almost exclusively due to DM annihilating to two gluons, so that $\sigma(\chi\bar{\chi} \to jj) \ll \sigma(\chi\bar{\chi} \to b\bar{b})$, while the annihilation into two light quarks is negligible. For $m_\chi \lesssim m_W$ and SM Yukawas, the required g_χ is thus
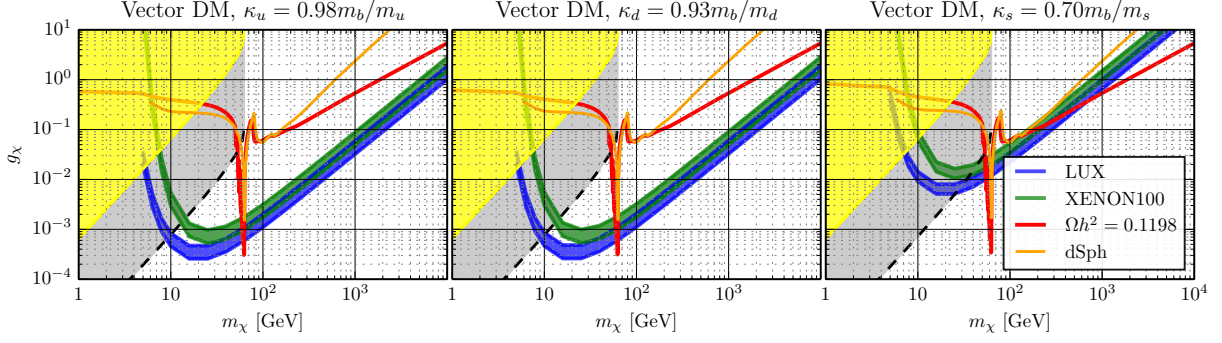
Figure 5: Bounds on the Higgs-portal coupling for vector DM, assuming maximal allowed values for the Yukawa couplings to the u, d, s quarks (left to right), keeping all the other couplings to their SM values. The color coding is the same as in Fig. 2.
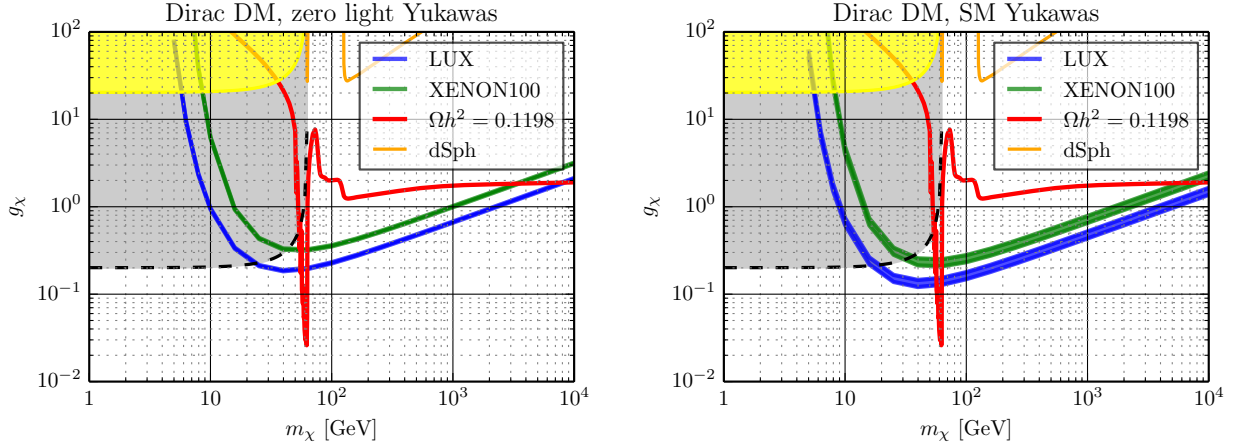

Figure 6: Bounds on the Higgs-portal coupling for Dirac DM, assuming $\Lambda = 1$ TeV and vanishing (left) and SM (right) Yukawa couplings to u, d, s quarks. The color coding is the same as in Fig. 2.

bigger by $30\% - 40\%$ than in the case of light Yukawas at their present experimental limits, and exhibits a significant jump below the b-quark threshold.
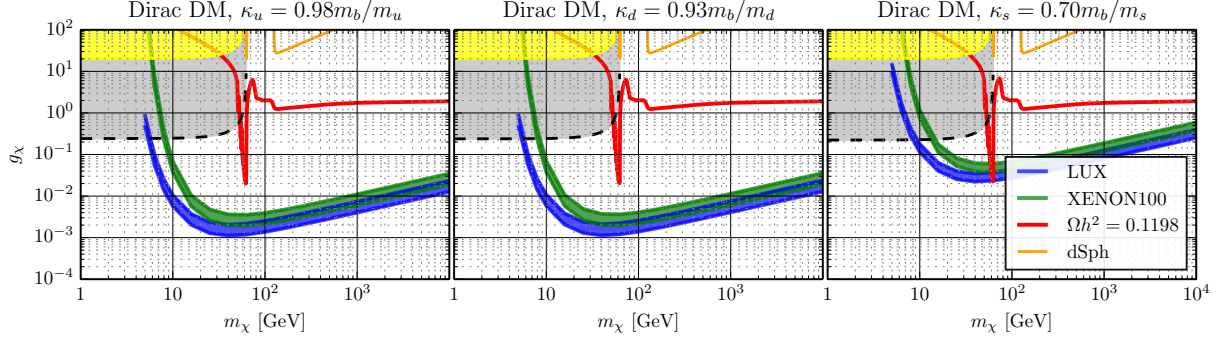
Figure 7: Bounds on the Higgs-portal coupling for Dirac DM, assuming $\Lambda = 1$ TeV and maximal allowed values for the Yukawa couplings to the u, d, s quarks (left to right), keeping all the other couplings to their SM values. The color coding is the same as in Fig. 2.
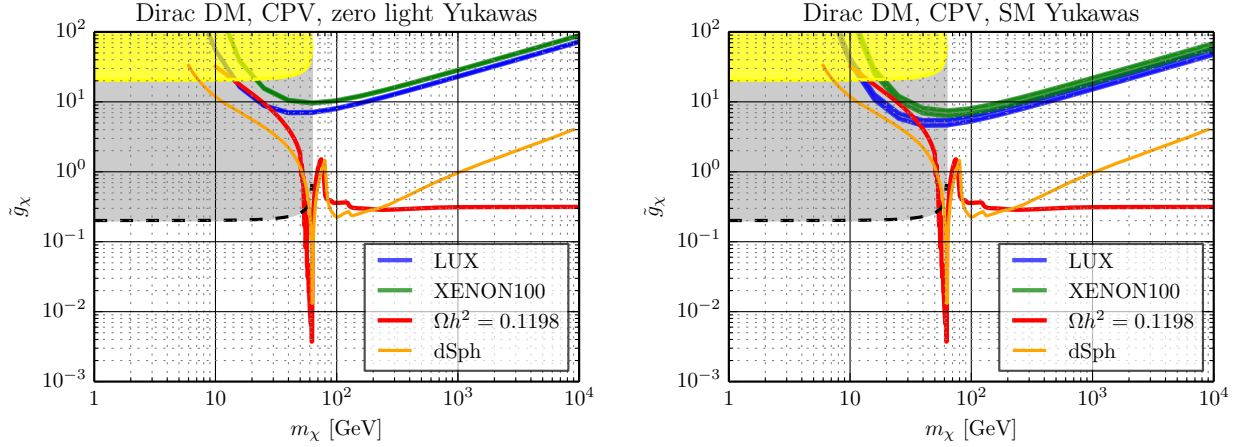

Figure 8: Bound on the pseudoscalar Higgs-portal coupling for Dirac DM, assuming $\Lambda = 1$ TeV and vanishing (left) and SM (right) Yukawa couplings to u, d, s quarks. The color coding is the same as in Fig. 2.
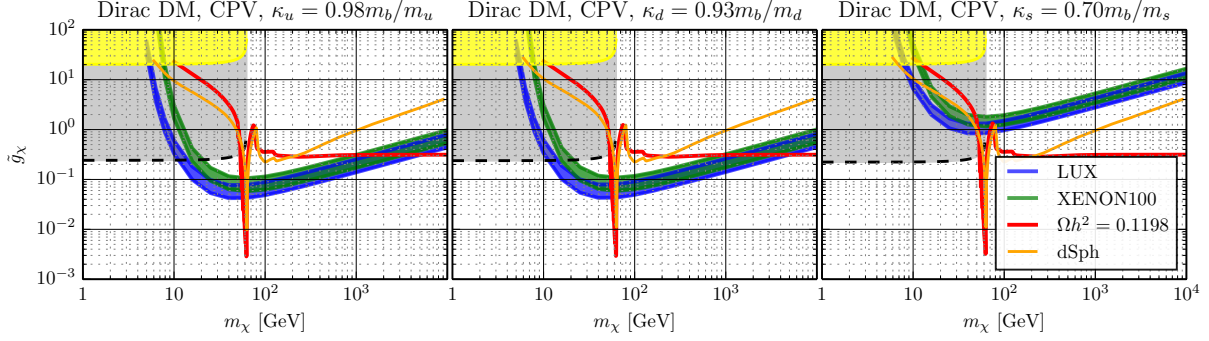
Figure 9: Bounds on the pseudoscalar Higgs-portal coupling for Dirac DM, assuming $\Lambda = 1$ TeV and maximal allowed values for the Yukawa couplings to the u, d, s quarks (left to right), keeping all the other couplings to their SM values. The color coding is the same as in Fig. 2.

C. Invisible decay width of the Higgs

The bounds on the invisible decay width of the Higgs boson provide stringent constraints on Higgs-portal DM [7]. The partial $h \to \chi\bar{\chi}$ decay widths are given by

$$
\begin{aligned}
\Gamma_{\chi\chi}^{S} &= \frac{g_\chi^2}{16\pi} \frac{v_W^2}{M_h} \beta_\chi \,, \\
\Gamma_{\chi\chi}^{DF} &= \frac{g_\chi^2}{8\pi} M_h \frac{v_W^2}{\Lambda^2} \beta_\chi^3 + \frac{\tilde{g}_\chi^2}{8\pi} M_h \frac{v_W^2}{\Lambda^2} \beta_\chi^{1/2} \,, \\
\Gamma_{\chi\chi}^{V} &= \frac{g_\chi^2}{128\pi} \frac{M_h^3 v_W^2}{m_\chi^4} \beta_\chi \left(1 - r_\chi + \tfrac{3}{4} r_\chi^2\right) \,,
\end{aligned}
\tag{17}
$$

where $r_\chi = 4m_\chi^2/M_h^2$ and $\beta_\chi = \sqrt{1 - r_\chi}$.

The current best limits on the invisible branching fraction of the SM Higgs are obtained from Zh production. The CMS collaboration gives a 95% CL limit of $\mathrm{Br}(h \to \mathrm{inv}) < 0.58$ for $M_h = 125$ GeV [42] and ATLAS finds $\mathrm{Br}(h \to \mathrm{inv}) < 0.75$ for $M_h = 125.5$ GeV [43]. Note that the increased light-quark Yukawa couplings, at their presently allowed values, do not appreciably change the Higgs production cross section [13]. Their main effect is to increase the total decay width of the Higgs and thus reduce the branching ratios to the other decay modes:

$$
\mathrm{Br}(h \to \chi\bar{\chi}) = \frac{\Gamma(h \to \chi\bar{\chi})}{\Gamma(h \to \chi\bar{\chi}) + \Gamma_h^{\mathrm{tot}} \times \left[1 + \sum_q (\kappa_q^2 - 1)\mathrm{Br}_{\mathrm{SM}}(h \to q\bar{q})\right]} \,.
\tag{18}
$$

In Figs. 2 to 9 we denote the bound on g_χ corresponding to the ATLAS upper limit on $\mathrm{Br}(h \to \mathrm{inv})$ with a dashed black line and grey out the excluded region in the g_χ vs. m_χ
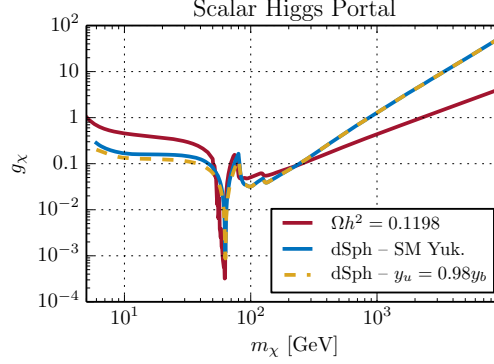
Figure 10: The effect of large light-quark Yukawa couplings on the indirect detection bounds from Fermi-LAT observations of Milky Way dwarf spheroidal satellite galaxies [45].

plane. We see that the light DM Higgs portal, $m_\chi \lesssim m_h/2$ is excluded by the Higgs invisible decay width.

Vector boson fusion, gluon fusion and $t\bar{t}H$ production, with the off-shell Higgs going to two DM particles, can provide some limited sensitivity to DM masses above $m_h/2$. A combination of the searches in the three channels at a 100 TeV collider could exclude the scalar thermal relic DM Higgs portal for DM masses in parts of the $m_h/2 \lesssim m_\chi \lesssim m_W$ interval at 95% C.L. [10] (these result receives only a negligible correction if light quark Yukawa couplings are enhanced). For $m_\chi < m_h/2$ the invisible Higgs decay width is, however, always the most constraining [44].

D. Indirect detection

In indirect signals of DM annihilation, the effect of changing the light-quark Yukawa couplings within the presently experimentally allowed ranges leads to at most $\mathcal{O}(1)$ effects. Further, the effect is present only for DM masses below the W threshold where the dominant annihilation channel is into the $b\bar{b}$ final state. For example, Fig. 10 shows the recast of the Fermi-LAT bound from dwarf spheroidals [45] for scalar DM, following the procedure outlined below.

Photon flux measurements with γ-ray telescopes can put a strong bound on the annihilation cross-section of the DM. The strongest bound in the DM mass range of interest has been recently released by the Fermi-LAT collaboration [45] based on `Pass 8` observation data of

the Milky Way dwarf spheroidal satellite galaxies (dSphs). There is also a recent analysis based on the Dark Energy Survey (DES) dSph candidates using the Fermi-LAT data [46]. While this bound is competitive with the one from the known dSphs, it is still weaker on its own. One could also consider the bounds from the isotropic gamma ray background (IGRB) [47]. In our analysis, we recast the Fermi-LAT bound on the $b\bar{b}$ final state using a simple re-weighting procedure of the photon spectra which will be discussed below.

The observed differential photon flux from the annihilation of dark matter is given by

$$\frac{d\Phi}{dE_\gamma d\Omega} = \frac{1}{4\pi} \frac{1}{2m_\chi^2} J \left[\sum_f \langle \sigma v \rangle_f \frac{dN_\gamma^f}{dE} \right], \tag{19}$$

where J is an astrophysical factor which depends on the distance to the source and the dark matter density profile. The factor in the brackets is the one most interesting for our purposes. It depends on the velocity-averaged cross-section and photon spectrum per DM annihilation.

The Fermi-LAT analysis gives bounds for the different final states separately while we have an admixture of final states. In order to recast the bound, we rely on the observation that for heavy DM the photon spectra from DM annihilation into quarks, gauge bosons, and the Higgs boson all peak at approximately the same photon energy and have approximately the same shape. Therefore, to extract the bound on the DM Higgs portal coupling g_χ, it is sufficient to find the zeros of the polynomial

$$f(g_\chi) = \sum_f \langle \sigma v \rangle_f \left(\frac{dN_\gamma^f}{dE} \right)^{\text{PEAK}} - \langle \sigma v \rangle_b^{\text{FERMI}} \left(\frac{dN_\gamma^b}{dE} \right)^{\text{PEAK}}, \tag{20}$$

where in the last term, $\langle \sigma v \rangle_b^{\text{FERMI}}$ is the bound from the Fermi-LAT analysis on the velocity-averaged cross-section. The photon spectra were obtained from the interpolation tables provided in the PPPC4DMID package [48]. In all cases except for the hh final state, $f(g_\chi)$ has only one zero up to a sign ambiguity. For the hh final state, however, the zero of $f(g_\chi)$ closest to the g_χ corresponding to $\chi\bar{\chi} \to b\bar{b}$ is the one used to rescale the Fermi-LAT bound on g_χ as a function of m_χ. The resulting bounds are shown in Figs. 2 to 9.

E. Direct detection

We have seen so far that most DM observables exhibit only a weak dependence on the light-quark Yukawas. This is not the case for the direct DM detection. In fact, modifying

the light-quark Yukawa couplings can significantly change the predictions for DM – nucleus scattering cross sections.

The differential cross section for spin-independent DM scattering on a nucleus is given by

$$\frac{d\sigma}{dE_R} = \frac{m_A}{\mu_{\chi A}^2 v_{\rm rel}^2} \frac{\overline{|\mathcal{M}|^2}}{32\pi s} \,, \tag{21}$$

where E_R is the nuclear recoil energy, m_A is the mass of the nucleus, $\mu_{\chi A} \equiv m_\chi m_A/(m_\chi + m_A)$ is the reduced mass of the DM – nucleus system, $s = (m_\chi + m_A)^2$ is the center-of-mass energy, $v_{\rm rel}$ is the DM velocity in the detector rest frame, and $\overline{|\mathcal{M}|^2}$ is the spin-averaged squared matrix element.

The matrix element $\mathcal{M}$ depends on the effective Higgs couplings to the nucleus. Since the momentum exchanges in DM scattering on nuclei are much smaller than the Higgs mass, we can calculate $\overline{|\mathcal{M}|^2}$ by first integrating out the Higgs and the heavy quarks (t, b, c). This gives an EFT with light quarks and gluons interacting with DM through local operators, described by the effective Lagrangians

$$\mathcal{L}_S = \frac{g_\chi v_W}{m_h^2} (\chi^\dagger \chi) \mathcal{S}_q \,, \tag{22}$$

$$\mathcal{L}_F = \frac{1}{\Lambda} \frac{g_\chi v_W}{m_h^2} (\bar{\chi}\chi) \mathcal{S}_q + \frac{1}{\Lambda} \frac{\tilde{g}_\chi v_W}{m_h^2} (\bar{\chi}i\gamma_5\chi) \mathcal{S}_q \,. \tag{23}$$

$$\mathcal{L}_V = \frac{g_\chi v_W}{2m_h^2} (\chi_\mu \chi^\mu) \mathcal{S}_q \,, \tag{24}$$

for scalar, fermion, and vector DM, respectively. The scalar current is the same in all three cases:

$$\mathcal{S}_q = \sum_q \kappa_q \frac{m_q}{v_W} \bar{q}q - \mathcal{C}_g \frac{\alpha_s}{12\pi v_W} G_{\mu\nu}^a G^{a\mu\nu} + \sum_q i\tilde{\kappa}_q \frac{m_q}{v_W} \bar{q}\gamma_5 q - \tilde{\mathcal{C}}_g \frac{\alpha_s}{8\pi v_W} G_{\mu\nu}^a \widetilde{G}^{a\mu\nu} \,. \tag{25}$$

Here, the last two terms arise from CP-violating Higgs couplings. The sums are over the light quarks $q = u, d, s$. The heavy quarks are integrated out and contribute only via the gluonic terms in the current. For the two corresponding dimensionless Wilson coefficients we have

$$\mathcal{C}_g = \kappa_g^{\rm NP} + \kappa_t + \kappa_b + \kappa_c \,, \qquad \tilde{\mathcal{C}}_g = \tilde{\kappa}_g^{\rm NP} + \tilde{\kappa}_t + \tilde{\kappa}_b + \tilde{\kappa}_c \,, \tag{26}$$

where the first contribution is from tree-level matching, and the remaining from one-loop matching, working in the limit of heavy quarks. This is well justified for top and bottom quarks. For scattering on heavy nuclei, e.g., on Xe or W, the maximal momentum exchanges

for DM with mass above approximately 1 TeV may, however, start to become comparable to the charm-quark mass. We neglect these effects, while they may need to be included in the future if such heavy DM is discovered.

CP-violating Higgs couplings to light quarks lead to spin-dependent interactions of DM with the target nuclei. The corresponding scattering rates are suppressed relative to the spin-independent interaction rates from CP-conserving Higgs couplings. We will therefore neglect the CP-violating interactions in our numerical analysis of direct detection scattering rates; i.e., we will set $\tilde{\kappa}_q = 0$, $\tilde{\mathcal{C}}_q = 0$ from now on.

The nucleon matrix elements of the remaining terms in the scalar current $\mathcal{S}_q$ are conventionally parametrized by (see, e.g., [49]),

$$\langle N|m_q\bar{q}q|N\rangle = m_N f_{Tq}^{(N)}\,, \tag{27}$$

$$\langle N|\frac{\alpha_s}{12\pi}G_{\mu\nu}G^{\mu\nu}|N\rangle = -\frac{2}{27}m_N f_{TG}^{(N)}\,. \tag{28}$$

In the heavy-quark limit for t, b, c the trace anomaly equation leads to the relation [49, 50]

$$f_{TG}^{(N)} = 1 - \sum_{q=u,d,s} f_{Tq}^{(N)}. \tag{29}$$

We can also define the effective Higgs coupling to nucleon as the expectation value of the scalar current,

$$f_{\mathcal{S}}^{(N)} \equiv \langle N|\mathcal{S}_q|N\rangle = \frac{m_N}{v_W}\left[\frac{2}{27}\mathcal{C}_g + \sum_q\left(\kappa_q - \frac{2}{27}\mathcal{C}_g\right)f_{Tq}^{(N)}\right]. \tag{30}$$

The exclusion curves from LUX [51] and Xenon100 [52], assuming a local DM density of 0.3 GeV/cm³, are shown in Figs. 2 to 9 as blue and red bands, respectively. The width of the exclusion curves represents the uncertainties in the hadronic matrix elements of the light-quark scalar currents. For the s quark we use the lattice determination $f_{Ts}^{(N)} = 0.043\pm$ 0.011 [53]. The matrix elements for u and d quarks can be related to the $\sigma_{\pi N}$ term. A Baryon Chiral Perturbation Theory (BχPT) analysis of the πN scattering data gives $\sigma_{\pi N} = 59(7)$ MeV [54]. This is in agreement with BχPT fit to world lattice $N_f = 2 + 1$ QCD data, which gives $\sigma_{\pi N} = 52(3)(8)$ MeV [55]. Including both $\Delta(1232)$ and finite spacing parametrization in the fit shifts the central value to $\sigma_{\pi N} = 44$MeV. To be conservative we use $\sigma_{\pi N} = (50 \pm 15)$MeV, which gives $f_{Tu}^{(p)} = (1.8 \pm 0.5) \times 10^{-2}$, $f_{Td}^{(p)} = (3.4 \pm 1.1) \times 10^{-2}$, $f_{Tu}^{(n)} = (1.6\pm 0.5) \times 10^{-2}$, $f_{Td}^{(n)} = (3.8\pm 1.1) \times 10^{-2}$, using the expressions in [56, 57]. For the

16

effective Higgs coupling to nucleons this gives

$$f_{\mathcal{S}}^{(p)} = \frac{m_W}{v_W}\Big[(1.8 \pm 0.5)\kappa_u + (3.4 \pm 1.1)\kappa_d + (4.3 \pm 1.1)\kappa_s$$
$$+ (6.70 \pm 0.12)\big(\kappa_c + \kappa_b + \kappa_t + \kappa_g^{\mathrm{NP}}\big)\Big] \times 10^{-2}\,, \tag{31}$$

$$f_{\mathcal{S}}^{(n)} = \frac{m_W}{v_W}\Big[(1.6 \pm 0.5)\kappa_u + (3.8 \pm 1.1)\kappa_d + (4.3 \pm 1.1)\kappa_s$$
$$+ (6.69 \pm 0.12)\big(\kappa_c + \kappa_b + \kappa_t + \kappa_g^{\mathrm{NP}}\big)\Big] \times 10^{-2}\,. \tag{32}$$

We use the results in [58] to relate the nuclear matrix elements to actual scattering rates on nuclei via nuclear form factors.

We show the direct detection exclusion limits for SM ($\kappa_{u,d,s} = 1$) or vanishing ($\kappa_{u,d,s} = 0$) light-quark Yukawa couplings in the right and left panels in Figs. 2, 4, 6, and 8, respectively. The exclusion limits are approximately two times weaker in the latter case; the constraint does not vanish because, for small values of the light-quark Yukawas, the scattering cross section is dominated by the gluon part of the scalar current, Eq. (25). When the light-quark Yukawas are taken to be at the upper limit of their experimentally allowed range, i.e. comparable to the SM bottom Yukawa, the direct detection bounds on g_χ become significantly stronger, by a factor of about m_b/m_q (Figs. 3, 5, 7, and 9).

It is interesting to note that, because of the dominance of the gluon contribution, for small light-quark Yukawas the theory uncertainty in the exclusion bands is significantly smaller than if the light Yukawa couplings are allowed to saturate the present experimental bounds. (The nuclear matrix element of the effective gluon term has smaller relative uncertainties than the corresponding matrix elements of $m_q \bar{q} q$ since $f_{TG}^{(N)} \gg f_{Tq}^{(N)}$.)

For m_χ smaller than a few TeV, the DM direct detection bounds are compatible with the thermal relic Higgs-portal DM only if light quark Yukawas are well below the present experimental bounds (the exception is a pseudoscalar fermion DM with enhanced strange Yukawa, where the bound is $m_\chi \gtrsim m_h/2$, see Fig. 9). This means that if thermal relic DM is discovered, it would immediately place an upper bound on $\kappa_u, \kappa_d, \kappa_s$, assuming Higgs-portal mediation (unless in the case of fermion DM that has purely pseudoscalar couplings). We comment in more detail on that observation in Section IV.

Since the DM – nucleus scattering cross section is the only DM observable that exhibits a rather pronounced dependence on the values of the light-quark Yukawas, we study this dependence in more detail.
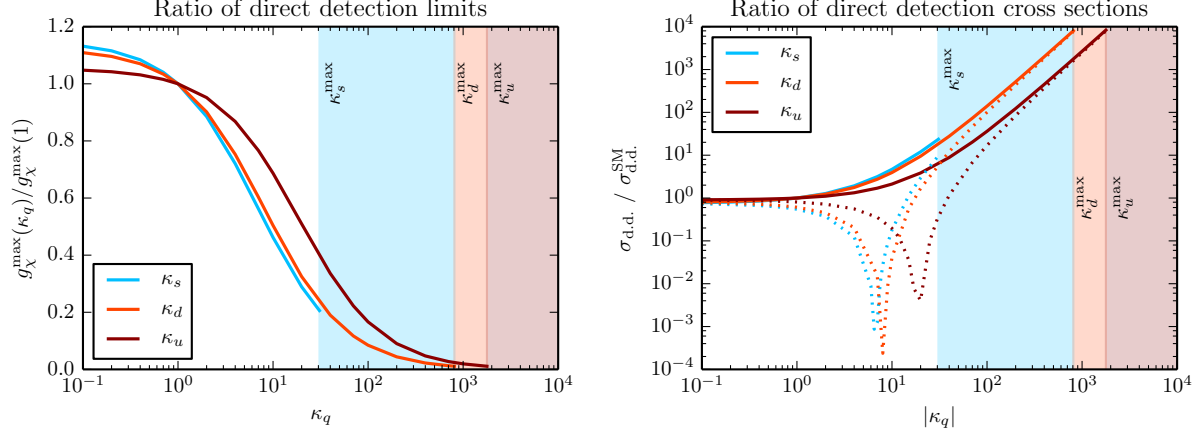
Figure 11: Left: The ratio of direct detection bounds on g_χ from Xenon target varying κ_u (dark red), κ_d (light red), or κ_s (blue), and the bound on g_χ assuming SM Higgs Yukawa couplings. The LHC upper bounds on κ_i are denoted by vertical dashed lines with shaded regions excluded. Right: the ratio of predicted scattering cross sections. The dotted lines correspond to negative values of κ_q.

In Fig. 11 (left) we show how the direct detection bounds on g_χ are affected by changes in the values of the light-quark Yukawas. We plot the ratio

$$\xi_{g_\chi} = \frac{g_\chi^{\max}(\kappa_q)}{g_\chi^{\max}(1)}, \tag{33}$$

where $g_\chi^{\max}(\kappa_q)$ is the upper bound on g_χ obtained from direct detection experiments for a given value of κ_q, with $q = u, d, s$. Hence, $g_\chi^{\max}(1)$ is the bound obtained assuming SM Yukawa couplings. Its value depends on m_χ, on whether DM is a scalar, fermion, or vector, and on the experiment that measured the bounds. Similarly, also $g_\chi^{\max}(\kappa_q)$ depends on m_χ, the spin of DM, and the experiment; however, all these dependences cancel in the ratio ξ_{g_χ}. The ratio ξ_{g_χ} thus only depends on κ_q and on which target material was used to derive the direct detection bounds. In Fig. 11 we show ξ_{g_χ} for a Xenon target, varying in turn κ_u (dark red line), κ_d (light red) and κ_s (blue), while keeping all other parameters fixed to their SM values. We set the hadronic matrix element $f_{Tq}^{(N)}$ to their present central values, anticipating that in the future their uncertainties will be further reduced. In Fig. 11 (right) we show a closely related quantity – the ratio of the scattering cross sections with varied $\kappa_{u,d,s}$ and the scattering cross section with SM Yukawa couplings, $\sigma_{\rm d.d.}/\sigma_{\rm d.d.}^{\rm SM}$.

Fig. 11 illustrates clearly that the difference between the bounds where one of the light quark Yukawa couplings is taken to be small or vanish completely, and the bounds where all the couplings are SM-like, is very small, $\mathcal{O}(10\%)$. Saturating the present experimental bounds on κ_u or κ_d, the allowed value of g_χ could lie two orders of magnitude below what one obtains for the case of SM Yukawa couplings. Such large values for the light-quark Yukawas are not very likely to be realized in a concrete model, as we will discuss in the next section. However, it is very interesting to observe that even a moderate increase of the values of the light-quark Yukawa couplings to only a few times their SM values can have a significant effect on the direct detection bounds, enhancing the scattering cross sections by up to a factor of ten.

Finally, in the right panel of Fig. 11 we show the cross section ratios for negative values of the κ_q (dotted lines). We see that the interference of the light-quark contributions with the effective gluon interaction can, in principle, lead to a strong reduction of the scattering cross section.

III. CHANGES TO YUKAWA COUPLINGS IN NEW PHYSICS MODELS

So far we allowed the Yukawa couplings of the Higgs to quarks to have arbitrary values, only restricting them to lie within the bounds obtained from global fits to LHC data. For simplicity, we also neglected flavor violation and CP violation when discussing their impact on the DM interactions.

Of course, changes of the Yukawa couplings by several orders of magnitude, as allowed by current experimental constraints on the light-quark Yukawas, are not very likely to be realized in a complete model, and might require significant fine tuning of the corresponding quark masses. In this section we investigate how large the deviations from the SM Yukawa interactions can be in popular models of NP with viable flavor structures.

Tables I and II summarize the predictions for the effective Yukawa couplings in the Standard Model (SM), in multi-Higgs-doublet models (MHDM) with natural flavor conservation (NFC) [59, 60], in the MSSM at tree level, the Giudice-Lebedev model of quark masses (GL) [61], in NP models with minimal flavor violation (MFV) [62], in Randall-Sundrum models (RS) [63], and in models with a composite Higgs, realized as a pseudo-Nambu-Goldstone boson (pNGB) [64–67]. For completeness, we include both the flavor-conserving

Model	κ_t	$\kappa_{c(u)}/\kappa_t$	$\tilde{\kappa}_t/\kappa_t$	$\tilde{\kappa}_{c(u)}/\kappa_t$
SM	1	1	0	0
NFC	$V_{hu}\, v_W/v_u$	1	0	0
MSSM	$\cos\alpha/\sin\beta$	1	0	0
GL	$1+\mathcal{O}(\epsilon^2)$	$\simeq 3(7)$	$\mathcal{O}(\epsilon^2)$	$\mathcal{O}(\kappa_{c(u)})$
GL2	$\cos\alpha/\sin\beta$	$\simeq 3(7)$	$\mathcal{O}(\epsilon^2)$	$\mathcal{O}(\kappa_{c(u)})$
MFV	$1+\frac{\mathrm{Re}(a_u v_W^2+2b_u m_t^2)}{\Lambda^2}$	$1-\frac{2\mathrm{Re}(b_u)m_t^2}{\Lambda^2}$	$\frac{\Im(a_u v_W^2+2b_u m_t^2)}{\Lambda^2}$	$\frac{\Im(a_u v_W^2)}{\Lambda^2}$
RS	$1-\mathcal{O}\!\left(\frac{v_W^2}{m_{KK}^2}\bar{Y}^2\right)$	$1+\mathcal{O}\!\left(\frac{v_W^2}{m_{KK}^2}\bar{Y}^2\right)$	$1+\mathcal{O}\!\left(\frac{v_W^2}{m_{KK}^2}\bar{Y}^2\right)$	$1+\mathcal{O}\!\left(\frac{v_W^2}{m_{KK}^2}\bar{Y}^2\right)$
pNGB	$1+\mathcal{O}\!\left(\frac{v_W^2}{f^2}\right)+\mathcal{O}\!\left(y_*^2\lambda^2\frac{v_W^2}{M_*^2}\right)$	$1+\mathcal{O}\!\left(y_*^2\lambda^2\frac{v_W^2}{M_*^2}\right)$	$\mathcal{O}\!\left(y_*^2\lambda^2\frac{v_W^2}{M_*^2}\right)$	$\mathcal{O}\!\left(y_*^2\lambda^2\frac{v_W^2}{M_*^2}\right)$

Table I: Predictions for the flavor diagonal up-type Yukawa couplings in a number of new physics models (see text for details).

and flavor-violating Yukawa interactions, and allow for CP violation. The Higgs couplings to quarks are thus described by

$$\mathcal{L}_{\text{eff,q}} = -\kappa_q \frac{m_q}{v_W}\bar{q}qh - i\tilde{\kappa}_q \frac{m_q}{v_W}\bar{q}\gamma_5 qh - \left[\left(\kappa_{qq'}+i\tilde{\kappa}_{qq'}\right)\bar{q}_L q'_R h + \text{h.c.}\right], \qquad (34)$$

where a sum over the SM quark fields is understood. The first two terms are flavor diagonal, with the first term CP conserving and the second term CP violating, and coincide with the definitions in eqs. (3) and (5), respectively. The terms in square brackets are flavor violating, with the real (imaginary) part of the coefficient CP conserving (violating). In the SM we have $\kappa_q = 1$, while $\tilde{\kappa}_q = \kappa_{qq'} = \tilde{\kappa}_{qq'} = 0$. The flavor-violating couplings in the above set of NP models are collected in Tables III and IV. These tables complement the analyses in [68–70] (see also [71], where implications of a negative top-quark Yukawa were explored, and [72] for an indirect bound on the down-quark Yukawa in alignment models).

A. Dimension-Six Operators with Minimal Flavor Violation

We start our discussion by considering dimension-six operators arising from integrating out NP at a high scale Λ. In addition, we assume that the flavor breaking in the NP sector is only due to the SM Yukawas, i.e. that NP satisfies the Minimal Flavor Violation (MFV) hypothesis [62, 73–78]. Integrating out the new physics states gives for the Higgs couplings

Model	κ_b	$\kappa_{s(d)}/\kappa_b$	$\tilde{\kappa}_b/\kappa_b$	$\tilde{\kappa}_{s(d)}/\kappa_b$
SM	1	1	0	0
NFC	$V_{hd}\,v_W/v_d$	1	0	0
MSSM	$-\sin\alpha/\cos\beta$	1	0	0
GL	$\simeq 3$	$\simeq 5/3(7/3)$	$\mathcal{O}(1)$	$\mathcal{O}(\kappa_{s(d)}/\kappa_b)$
GL2	$-\sin\alpha/\cos\beta$	$\simeq 3(5)$	$\mathcal{O}(\epsilon^2)$	$\mathcal{O}(\kappa_{s(d)}/\kappa_b)$
MFV	$1+\dfrac{\mathrm{Re}(a_d v_W^2+2c_d m_t^2)}{\Lambda^2}$	$1-\dfrac{2\mathrm{Re}(c_d)m_t^2}{\Lambda^2}$	$\dfrac{\Im(a_d v_W^2+2c_d m_t^2)}{\Lambda^2}$	$\dfrac{\Im(a_d v_W^2+2c_d|V_{ts(td)}|^2 m_t^2)}{\Lambda^2}$
RS	$1-\mathcal{O}\left(\dfrac{v_W^2}{m_{KK}^2}\bar{Y}^2\right)$	$1+\mathcal{O}\left(\dfrac{v_W^2}{m_{KK}^2}\bar{Y}^2\right)$	$1+\mathcal{O}\left(\dfrac{v_W^2}{m_{KK}^2}\bar{Y}^2\right)$	$1+\mathcal{O}\left(\dfrac{v_W^2}{m_{KK}^2}\bar{Y}^2\right)$
pNGB	$1+\mathcal{O}\left(\dfrac{v_W^2}{f^2}\right)+\mathcal{O}\left(y_*^2\lambda^2\dfrac{v_W^2}{M_*^2}\right)$	$1+\mathcal{O}\left(y_*^2\lambda^2\dfrac{v_W^2}{M_*^2}\right)$	$\mathcal{O}\left(y_*^2\lambda^2\dfrac{v_W^2}{M_*^2}\right)$	$\mathcal{O}\left(y_*^2\lambda^2\dfrac{v_W^2}{M_*^2}\right)$

Table II: Predictions for the flavor diagonal down-type Yukawa couplings in a number of new physics models (see text for details).

Model	$\kappa_{ct(tc)}/\kappa_t$	$\kappa_{ut(tu)}/\kappa_t$	$\kappa_{uc(cu)}/\kappa_t$
GL & GL2	$\epsilon(\epsilon^2)$	$\epsilon(\epsilon^2)$	ϵ^3
MFV	$\dfrac{\mathrm{Re}\left(c_u m_b^2 V_{cb}^{(*)}\right)}{\Lambda^2}\dfrac{\sqrt{2}m_{t(c)}}{v_W}$	$\dfrac{\mathrm{Re}\left(c_u m_b^2 V_{ub}^{(*)}\right)}{\Lambda^2}\dfrac{\sqrt{2}m_{t(u)}}{v_W}$	$\dfrac{\mathrm{Re}\left(c_u m_b^2 V_{ub(cb)}V_{cb(ub)}^*\right)}{\Lambda^2}\dfrac{\sqrt{2}m_{c(u)}}{v_W}$
RS	$\sim\lambda^{(-)2}\dfrac{m_{t(c)}}{v_W}\bar{Y}^2\dfrac{v_W^2}{m_{KK}^2}$	$\sim\lambda^{(-)3}\dfrac{m_{t(u)}}{v_W}\bar{Y}^2\dfrac{v_W^2}{m_{KK}^2}$	$\sim\lambda^{(-)1}\dfrac{m_{c(u)}}{v_W}\bar{Y}^2\dfrac{v_W^2}{m_{KK}^2}$
pNGB	$\mathcal{O}(y_*^2\dfrac{m_t}{v_W}\dfrac{\lambda_{L(R),2}\lambda_{L(R),3}m_W^2}{M_*^2})$	$\mathcal{O}(y_*^2\dfrac{m_t}{v_W}\dfrac{\lambda_{L(R),1}\lambda_{L(R),3}m_W^2}{M_*^2})$	$\mathcal{O}(y_*^2\dfrac{m_c}{v_W}\dfrac{\lambda_{L(R),1}\lambda_{L(R),2}m_W^2}{M_*^2})$

Table III: Predictions for the flavor violating up-type Yukawa couplings in a number of new physics models (see text for details). In the SM, NFC and the tree-level MSSM the Higgs Yukawa couplings are flavor diagonal. The estimates of the CP-violating versions of the flavor-changing transitions, κ_{ij}/κ_t, are the same as the CP-conserving ones, apart from substituting "Im" for "Re" in the "MFV" row.

to quarks

$$\mathcal{L}_{\mathrm{EFT}} = Y_u\bar{Q}_L H^c u_R + Y_d\bar{Q}_L H d_R + \frac{Y'_u}{\Lambda^2}\bar{Q}_L H^c u_R(H^\dagger H) + \frac{Y'_d}{\Lambda^2}\bar{Q}_L H d_R(H^\dagger H) + \mathrm{h.c.}\,, \quad (35)$$

where Λ is the scale of new physics and $H^c = i\sigma_2 H^*$. We identify the NP scales in the up- and down-quark sectors for simplicity. There are also modifications of quark kinetic terms through dimension-six derivative operators. These can be absorbed in (35) using equations

Model	$\kappa_{bs(sb)}/\kappa_b$	$\kappa_{bd(db)}/\kappa_b$	$\kappa_{sd(ds)}/\kappa_b$
GL & GL2	$\epsilon^3(\epsilon^2)$	ϵ^2	$\epsilon^3(\epsilon^4)$
MFV	$\frac{\mathrm{Re}\left(c_d m_t^2 V_{ts}^{(*)}\right)}{\Lambda^2}\frac{\sqrt{2}m_{s(b)}}{v_W}$	$\frac{\mathrm{Re}\left(c_d m_t^2 V_{td}^{(*)}\right)}{\Lambda^2}\frac{\sqrt{2}m_{d(b)}}{v_W}$	$\frac{\mathrm{Re}\left(c_d m_t^2 V_{ts(td)}^* V_{td(ts)}\right)}{\Lambda^2}\frac{\sqrt{2}m_{s(d)}}{v_W}$
RS	$\sim \lambda^{(-)2}\frac{m_{b(s)}}{v_W}\bar{Y}^2\frac{v_W^2}{m_{KK}^2}$	$\sim \lambda^{(-)3}\frac{m_{b(d)}}{v_W}\bar{Y}^2\frac{v_W^2}{m_{KK}^2}$	$\sim \lambda^{(-)1}\frac{m_{s(d)}}{v_W}\bar{Y}^2\frac{v_W^2}{m_{KK}^2}$
pNGB	$\mathcal{O}(y_*^2\frac{m_b}{v_W}\frac{\lambda_{L(R),2}\lambda_{L(R),3}m_W^2}{M_*^2})$	$\mathcal{O}(y_*^2\frac{m_b}{v_W}\frac{\lambda_{L(R),1}\lambda_{L(R),3}m_W^2}{M_*^2})$	$\mathcal{O}(y_*^2\frac{m_s}{v_W}\frac{\lambda_{L(R),1}\lambda_{L(R),2}m_W^2}{M_*^2})$

Table IV: Predictions for the flavor violating down-type Yukawa couplings in a number of new physics models (see text for details). In SM, NFC and tree level MSSM the Higgs Yukawa couplings are flavor diagonal. The estimates of the CP-violating versions of the flavor-changing transitions, κ_{ij}/κ_b, are the same as the CP-conserving ones, apart from substituting "Im" for "Re" in the "MFV" row.

of motion [79]. The quark mass matrices and Yukawa couplings after EWSB are thus

$$M_q = \frac{v_W}{\sqrt{2}}\left(Y_q + Y_q'\frac{v_W^2}{2\Lambda^2}\right), \qquad y_q = Y_q + 3Y_q'\frac{v_W^2}{2\Lambda^2}, \qquad q = u,d. \qquad (36)$$

Because Y_q and $Y_{q'}$ appear in two different combinations in M_q and y_q, the two, in general, cannot be made diagonal in the same basis.

In MFV the coefficients of the dimension-six operators can be expanded in terms of $Y_{u,d}$,

$$\begin{aligned} Y_u' &= a_u Y_u + b_u Y_u Y_u^\dagger Y_u + c_u Y_d Y_d^\dagger Y_u + \cdots, \\ Y_d' &= a_d Y_d + b_d Y_d Y_d^\dagger Y_d + c_d Y_u Y_u^\dagger Y_d + \cdots. \end{aligned} \qquad (37)$$

with $a_q, b_q, c_q \sim \mathcal{O}(1)$. Working to first order in dimension-six operator insertions we can thus write for the Yukawa couplings, in the mass eigenbases for up and down quarks respectively,

$$\begin{aligned} y_u &= \left[1 + \frac{v_W^2}{\Lambda^2}\left(a_u + b_u(y_{\mathrm{SM}}^u)^2 + c_u V(y_{\mathrm{SM}}^d)^2 V^\dagger + \cdots\right)\right]y_{\mathrm{SM}}^u, \\ y_d &= \left[1 + \frac{v_W^2}{\Lambda^2}\left(a_d + b_d(y_{\mathrm{SM}}^d)^2 + c_d V^\dagger(y_{\mathrm{SM}}^u)^2 V + \cdots\right)\right]y_{\mathrm{SM}}^d. \end{aligned} \qquad (38)$$

Here $y_{\mathrm{SM}}^{u,d}$ are the diagonal matrices of the SM Yukawa couplings, while V is the Cabibbo-Kobayashi-Maskawa (CKM) matrix. In general, the coefficients a_q, b_q, c_q are complex so that CP-violating Higgs couplings arise at $\mathcal{O}(v_W^2/\Lambda^2)$. Flavor-violating Higgs couplings arise first from the terms proportional to $c_{u,d}$ in the Yukawa expansion and are thus suppressed by the corresponding CKM matrix elements. In Tables I-IV we collect the values for flavor-conserving and flavor-violating Yukawa couplings in the "MFV" row, assuming that all the

coefficients a_q, b_q, c_q are $\mathcal{O}(1)$, and show only the numerically leading non-SM contributions. In the expressions we also set V_{tb} to unity.

The corrections to DM phenomenology are dominated by changes of the third-generation Yukawa couplings. The MFV corrections to light-quark Yukawa couplings are all either additionally CKM suppressed or involve extra insertions of light-quark masses. Hence the theory error in Higgs-portal DM phenomenology due to Yukawa coupling uncertainties will be small in MFV models of NP once the Higgs couplings to top and bottom quarks are well measured.

B. Multi-Higgs-doublet model with natural flavor conservation

In MHDMs there are no tree-level FCNCs if natural flavor conservation is assumed [59, 60]. Under this assumption we can choose a Higgs doublet basis in which only one doublet, H_u, couples to the up-type quarks, and only one Higgs doublet, H_d, couples to the down-type quarks[2]. After EWSB the two doublets obtain the vevs v_u and v_d, respectively. On the other hand, the vevs of all Higgs doublets contribute to the W and Z masses. They satisfy the sum rule $v_W^2 = \sum_i v_i^2$, where the sum is over all Higgs doublets.

The neutral scalar components of H_i are $(v_i + h_i)/\sqrt{2}$, where the dynamical fields h_i are a linear combination of the neutral Higgs mass eigenstates (and include h_u and h_d). We thus have $h_i = V_{hi}h + \ldots$, where V_{hi} are elements of the unitary matrix V that diagonalizes the neutral-Higgs mass terms and we only write down the contribution of the lightest Higgs, h. Under the assumptions above, the mass and Yukawa terms can be diagonalized in the same basis, so that there is no flavor violation and no CP violation in the Yukawa interactions:

$$\kappa_{qq'} = \tilde{\kappa}_{qq'} = 0 , \qquad \tilde{\kappa}_q = 0 . \tag{39}$$

We obtain a universal shift in all up-quark Yukawa couplings, and a different universal shift in all down-quark Yukawa couplings, given by

$$\kappa_u = \kappa_c = \kappa_t = V_{hu}\frac{v_W}{v_u} , \qquad \kappa_d = \kappa_s = \kappa_b = V_{hd}\frac{v_W}{v_d} . \tag{40}$$

Since the shifts are universal over generations, the precise measurements of the Higgs couplings to top and bottom quarks will also determine the Higgs couplings to light quarks.

---

[2] Note that $H_u = H_d$ is included as a special case.

Both κ_t and κ_b are expected to be known with $\mathcal{O}(5\%)$ precision after the end of the high-luminosity LHC run [80, 81]. The uncertainties in the DM direct detection rates due to uncertainties in the Yukawa couplings will thus be negligible, assuming NFC. Note that the Higgs portal with an additional SM singlet mixing with the Higgs is also described by the above modifications of fermion couplings, with a completely universal shift $\kappa_i = \cos\theta$, where θ is the singlet–Higgs mixing angle [82, 83].

Our analysis of modified Higgs-portal DM phenomenology given in Section II applies in the somewhat special limit where the DM only couples to the lightest mass-eigenstate h. For instance, for scalar DM the general Higgs portal is

$$\mathcal{L}_{\mathrm{NFC}} = g_{\chi,ij} \chi^\dagger \chi H_i^\dagger H_j. \tag{41}$$

If the hermitian matrix of couplings $g_{\chi,ij}$ is such that it has h as the only eigenstate with nonzero eigenvalue, then our analysis in Section II applies unchanged. In general, however, all the expressions in Section II get corrected by terms of order $1/m_{H_i}^2$ due to exchanges of heavy Higgs bosons with masses m_{H_i}. If DM is heavy, $m_\chi > m_{H_i}$, the presence of heavy Higgs bosons would also open new annihilation channels.

C. Type-II Two-Higgs-Doublet Model

The MSSM tree-level Higgs potential and the couplings to quarks are the same as in the type-II two-Higgs-doublet model (2HDM), see, e.g., [84]. This is an example of a 2HDM with natural flavor conservation in which $v_u = \sin\beta\, v_W$, $v_d = \cos\beta\, v_W$. The mixing of $h_{u,d}$ into the Higgs mass-eigenstates h and H is given by

$$\begin{pmatrix} h_u \\ h_d \end{pmatrix} = \begin{pmatrix} \cos\alpha & \sin\alpha \\ -\sin\alpha & \cos\alpha \end{pmatrix} \begin{pmatrix} h \\ H \end{pmatrix}, \tag{42}$$

where h is the observed SM-like Higgs. Thus

$$\begin{aligned}
\kappa_u = \kappa_c = \kappa_t = \frac{\cos\alpha}{\sin\beta}, \\
\kappa_d = \kappa_s = \kappa_b = -\frac{\sin\alpha}{\cos\beta},
\end{aligned} \tag{43}$$

while the flavor-violating and/or CP-violating Yukawas are zero. In the decoupling limit $(\beta - \alpha = \pi/2)$ the heavy Higgs bosons become infinitely heavy, while the Yukawa couplings

tend toward their SM value, $\kappa_i = 1$. The global fits to Higgs data in type-II 2HDM already constrain $\beta - \alpha \simeq \pi/2$ [37, 85, 86] so that in this case the corrections to Higgs-portal DM phenomenology due to non-standard Higgs Yukawa couplings are small.

As in the case of MHDM, the DM phenomenology of Section II remains unchanged only in the limit where the DM couples to the light Higgs h but not to the heavy Higgs H. In the general case, our analysis gets corrections that are relatively suppressed by $\mathcal{O}(m_h^2/m_H^2)$. If we are not too far away from the decoupling limit these corrections can be neglected, while in parts of the parameter space, where cancellation can occur, the extra contributions are numerically important [8].

D. Higgs-dependent Yukawa Couplings

In the model of quark masses introduced by Giudice and Ledebev (GL) [61] the Higgs-quark interactions are written in terms of effective operators

$$\mathcal{L}_q = c_{ij}^u \left(\frac{H^\dagger H}{M^2} \right)^{n_{ij}^u} \bar{Q}_{L,i} u_{R,j} H^c + c_{ij}^d \left(\frac{H^\dagger H}{M^2} \right)^{n_{ij}^d} \bar{Q}_{L,i} d_{R,j} H + \text{h.c.} . \tag{44}$$

They can be thought of as arising from integrating out heavy mediators at a large mass scale M. In this model the light quarks couple to the Higgs only through operators with mass dimension higher than four, i.e., for light quarks we have $n_{ij}^{u,d} \neq 0$. The values of the integers $n_{ij}^{u,d}$, and of the coefficients $c_{ij}^{u,d}$ that take values of order unity, are chosen such that the hierarchies of the observed quark masses and mixing angles are explained, after EWSB, in terms of the expansion parameter $\epsilon \equiv v_W^2/M^2 \approx 1/60$. Thus, the Yukawa couplings are of the form

$$y_{ij}^{u,d} = (2n_{ij}^{u,d} + 1)(y_{ij}^{u,d})_{\text{SM}} . \tag{45}$$

After mass diagonalization the SM Yukawas are diagonal in the same basis as the quark masses, $(y_{ij}^{u,d})_{\text{SM}} \propto \delta_{ij} m_i^{u,d}$, while the $y_{ij}^{u,d}$ are not diagonal in the same basis[3]. Using the ansatz $n_{ij}^{u,d} = a_i + b_j^{u,d}$ with $a = (1,1,0)$, $b^d = (2,1,1)$, and $b^u = (2,0,0)$, this gives the deviations in the Yukawa couplings collected in Tables I-IV in the row denoted by "GL". Since the couplings to the bottom quark is enhanced by a large factor, $\kappa_b \simeq 3$, the simplest

---

[3] Note that the mixing of contributions from different effective operators that may have large relative phases could lead to sizeable CP-violating contributions to the Yukawa couplings.

version of the GL model is already excluded by the Higgs data on $h \to WW$, $h \to ZZ$ and $h \to \gamma\gamma$ decays.

We therefore modify the initial GL proposal and assume that we have two Higgs doublets in (44), H_u that only gives masses to up-type quarks and H_d that only gives masses to down-type quarks. The correct mass and CKM angle hierarchy is obtained by using $b^d = (1, 0, 0)$ in the ansatz for n_{ij}^d, and leaving a and b^u unchanged. This gives satisfactory Higgs phenomenology at present as long as $\kappa_b = \sin\alpha/\cos\beta \simeq 1$ up to $\mathcal{O}(20\%)$. In this limit also $\kappa_t = \cos\alpha/\sin\beta \simeq 1$. The scaling of Yukawa couplings for this modification of the GL model is shown in Tables I-IV in the row denoted by "GL2".

In the GL model it is natural that the Higgs is the only state that couples to DM. The GL model is thus an example of Higgs-portal DM where the light-quark Yukawa couplings can substantially differ from their SM values. For instance, in GL2 $\kappa_u \simeq 7\kappa_t$, $\kappa_d \simeq 5\kappa_b$, $\kappa_s \simeq 3\kappa_b$, $\kappa_c \simeq 3\kappa_t$. The coupling of DM to gluons (25) $\mathcal{C}_g \simeq 4\kappa_t + \kappa_b$, so that $\mathcal{C}_g \sim (5/3)\mathcal{C}_g^{\mathrm{SM}}$, and $\tilde{\mathcal{C}}_g \sim \mathcal{O}(\mathcal{C}_g)$. Taking $\kappa_b \simeq 1$, this means that the effective Higgs coupling to nucleons, governing the direct DM detections rates, gets enhanced compared to the SM Higgs Yukawa couplings by

$$\frac{f_{\mathcal{S}}^{(p)}}{f_{\mathcal{S}}^{(p)}|_{\mathrm{SM}}} \simeq 1.2\kappa_t + 1.3\kappa_b \simeq 2.5 \,, \qquad \frac{f_{\mathcal{S}}^{(n)}}{f_{\mathcal{S}}^{(n)}|_{\mathrm{SM}}} \simeq 1.3\kappa_t + 1.3\kappa_b \simeq 2.6 \,. \qquad (46)$$

Here most of the enhancement over the SM comes from enhanced κ_u and κ_d, which is also the reason for enlarged isospin breaking (the difference between $f_{\mathcal{S}}^{(p)}$ and $f_{\mathcal{S}}^{(n)}$). As a result of larger couplings to light quarks the spin-independent DM scattering cross section can thus be enhanced by an order of magnitude in the GL2 model of light-quark masses.

E. Randall-Sundrum models

The Randall-Sundrum (RS) warped extra-dimensional models with the SM fields propagating in the bulk provide a solution to the hierarchy problem and simultaneously explain the hierarchy of the SM fermion masses without large hierarchies in the initial five-dimensional (5D) Lagrangian [63, 87, 88]. The fermion zero modes are either localized toward the UV brane (for lighter fermions) or toward the IR brane (the top, the left-handed b quark and potentially the right-handed c quark) [89, 90]. The Higgs field and the Higgs vev are both localized toward the IR brane. Integrating out the Kaluza-Klein (KK) modes and working

26

in the limit of a brane-localized Higgs, the SM quark mass matrices are given, to leading order in v_W^2/m_{KK}^2, by [91] (see also [92–100], and Ref. [101] for a bulk Higgs scenario)

$$M_{ij}^{d(u)} = \left[F_q Y_{1(2)}^{5D} F_{d(u)}\right]_{ij} v_W \,. \tag{47}$$

Here, m_{KK} is the KK mass scale. The $F_{q,u,d}$ are diagonal 3×3 matrices of fermion wave-functions for the left-handed electroweak quark doublets and the right-handed electroweak up and down quark singlets, respectively, evaluated at the IR brane. Assuming flavor anarchy, the 5D Yukawa matrices for up and down quarks, $Y_{1,2}^{5D}$, are general 3×3 complex matrices with $\mathcal{O}(1)$ entries. For a Higgs field propagating in the bulk, 5D gauge invariance guarantees $Y_1^{5D} = Y_2^{5D}$ [91].

At leading order in v_W^2/m_{KK}^2 the Higgs Yukawas are aligned with the quark masses, i.e.,

$$M_{u,d} = y_{u,d} \frac{v_W}{\sqrt{2}} + \mathcal{O}(v_W^2/m_{KK}^2) \,. \tag{48}$$

The misalignment arises from dimension-six operators that are generated by tree-level KK quark exchanges. They give

$$\left[y_{u(d)}\right]_{ij} - \frac{\sqrt{2}}{v_W}\left[M_{u,d}\right]_{ij} \sim -\frac{2}{3} F_{q_i} \bar{Y}^3 F_{u_j(d_j)} \frac{v_W^2}{m_{KK}^2} \,, \tag{49}$$

where $\bar{Y}$ is a typical value of the dimensionless 5D Yukawa coupling and is in numerical analyses typically taken to be below $\bar{Y} \lesssim 4$ (see, e.g., [95]). The Higgs mediated FCNCs are thus suppressed by the same zero-mode wave-function overlaps that also suppress the quark masses, giving rise to the RS GIM mechanism [102–104].

Using that the CKM matrix elements are given by $V_{ij} \sim F_{q_i}/F_{q_j}$ for $i < j$, Eq. (49) can be rewritten as

$$\left[y_{u(d)}\right]_{ij} - \frac{\sqrt{2}}{v_W}\left[M_{u,d}\right]_{ij} \sim -\frac{2}{3} \bar{Y}^2 \frac{v_W^2}{m_{KK}^2} \begin{cases} \frac{m_{u_j(d_j)}}{v_W} V_{ij} \,, & i < j \,, \\ 1 \,, & i = j \,, \\ \frac{m_{u_i(d_i)}}{v_W} V_{ij}^{-1} \,, & j < i \,. \end{cases} \tag{50}$$

This yields the κ_i collected in Tables I-IV. In the numerical analysis of ref. [91] the diagonal values κ_i were typically found to be smaller than one, with deviations in κ_t up to 30%, κ_b up to 15%, in $\kappa_{s,c}$ up to $\sim 5\%$, and in $\kappa_{u,d}$ of 1% (these estimates were obtained fixing the mass of the first KK gluon excitation to 3.7 TeV, above the present ATLAS bound [105]). The effective Higgs coupling to nucleons, $f_{\mathcal{S}}^{(N)}$, thus only gets reduced by $\mathcal{O}(10\%)$,

giving a $\mathcal{O}(20\%)$ smaller DM scattering cross section on nuclei, compared to the case of SM Yukawa couplings. The largest effect arises in DM annihilations to top quarks, where the cross section can be reduced by a factor of two, while the annihilation cross section to $b\bar{b}$ pairs can be $\sim 30\%$ smaller than for SM Yukawa couplings.

F. Composite pseudo-Goldstone Higgs

Finally, we investigate the possibility that the Higgs is a pseudo-Goldstone boson arising from the spontaneous breaking of a global symmetry in a strongly coupled sector [64–67]. We assume that the SM fermions couple linearly to composite operators $O_{L,R}$ [106],

$$\lambda^q_{L,i}\bar{Q}_{L,i}O^i_R + \lambda^u_{R,j}\bar{u}_{R,j}O^j_L + h.c.,\tag{51}$$

where i, j are flavor indices. This is the 4D dual of the fermion mass generation in 5D RS models. The Higgs couples to the composite sector with a typical coupling y_*. The SM masses and Yukawa couplings then arise from expanding the two-point functions of the $O_{L,R}$ operators in powers of the Higgs field [107], giving rise to four- and higher-dimensional Higgs operators, such as in (35).

The new ingredient, related to the pNGB nature of the Higgs, is that the shift symmetry dictates the form of the higher-dimensional operators. The flavor structure and the composite Higgs coset structure completely factorize if the SM fields couple to only one composite operator. The general decomposition of Higgs couplings then becomes [107] (see also [108, 109])

$$Y_u\bar{Q}_L H u_R + Y'_u\bar{Q}_L H u_R \frac{(H^\dagger H)}{\Lambda^2} + \dots \quad \to \quad c^u_{ij}\,P(h/f)\,\bar{Q}^i_L H u^j_R,\tag{52}$$

and similarly for the down quarks. Here $P(h/f) = a_0 + a_2(h/f)^2 + \dots$ is an analytic function whose form is fixed by the structure of the spontaneous breaking and the embedding of the SM fields in the global symmetry of the strongly coupled sector, while f is the equivalent of the pion decay constant and is of order v_W. Since the flavor structure of the coefficients of the dimension-four and dimension-six operators is the same, they can be diagonalized simultaneously. All corrections to the quark Yukawa couplings from this effect are therefore strictly diagonal, and we have

$$\kappa_q \sim 1 + \mathcal{O}\Big(\frac{v_W^2}{f^2}\Big).\tag{53}$$

For example, for the models based on the breaking of $SO(5)$ to $SO(4)$, the diagonal Yukawa couplings can be written as [110]

$$\kappa_q = \frac{1 + 2m - (1 + 2m + n)(v_W/f)^2}{\sqrt{1 - (v_W/f)^2}}, \tag{54}$$

where n, m are positive integers. The MCHM4 model corresponds to $m = n = 0$, while MCHM5 is given by $m = 0, n = 1$.

The flavor-violating contributions to the quark Yukawa couplings then arise only from corrections to the quark kinetic terms. That is, they are related to dimension-six operators of the form [107]

$$\bar{q}_L i \slashed{D} q_L \frac{H^\dagger H}{\Lambda^2}, \ \bar{u}_R i \slashed{D} u_R \frac{H^\dagger H}{\Lambda^2}, \dots . \tag{55}$$

These operators arise from the exchange of composite vector resonances with typical mass $M_* \sim \Lambda$. After using the equations of motion they contribute to the misalignment between the fermion masses and the corresponding Yukawa couplings. The NDA estimates for these corrections are, neglecting relative $\mathcal{O}(1)$ contributions in the sum [15, 107, 111],

$$\kappa_{ij}^u \sim 2y_*^2 \frac{v_W^2}{M_*^2} \left(\lambda_{L,i}^q \lambda_{L,j}^q \frac{m_{u_j}}{v_W} + \lambda_{R,i}^u \lambda_{R,j}^u \frac{m_{u_i}}{v_W} \right), \tag{56}$$

and similarly for the down quarks. If the strong sector is CP violating, then $\tilde{\kappa}_{ij}^{u,d} \sim \kappa_{ij}^{u,d}$.

The exchange of composite vector resonances contributes also to the flavor diagonal Yukawa couplings, shifting the estimate (53) by (note the different normalizations of κ_q and $\kappa_{qq'}$ in (34))

$$\Delta \kappa_{q_i} \sim 2y_*^2 \frac{v_W^2}{M_*^2} \left[\left(\lambda_{L,i}^q \right)^2 + \left(\lambda_{R,i}^u \right)^2 \right]. \tag{57}$$

This shift can be large for the quarks with a large composite component if the Higgs is strongly coupled to the vector resonances, $y_* \sim 4\pi$, and these resonances are relatively light, $M_* \sim 4\pi v_W \sim 3$ TeV. The left-handed top and bottom, as well as the right-handed top, are expected to be composite, explaining the large top mass (i.e., $\lambda_{L,3}^q \sim \lambda_{R,3}^u \sim 1$). In the anarchic flavor scenario, one expects the remaining quarks to be mostly elementary (so the remaining $\lambda_i \ll 1$). However, if there is some underlying flavor alignment, it is also possible that the light quarks are composite. This is most easily achieved in the right-handed sector [109, 112, 113]. Taking all right-handed up-type quarks fully composite, and assuming that this results in a shift $\Delta \kappa_u \sim \Delta \kappa_c \sim \Delta \kappa_t \sim 1$, this would lead to an increase in the effective Higgs coupling to nucleons, $f_{\mathcal{S}}^{(N)}$, of about 50%, and an increase in the DM-nucleon scattering rate of about 100%.

IV. CONSTRAINING THE LIGHT-QUARK YUKAWA COUPLINGS

If DM is a thermal relic interacting with ordinary matter predominantly via SM Higgs exchange, direct detection scattering rates immediately give information about the light-quark Yukawa couplings once the coupling of the DM particle to the Higgs particle is fixed.

In fact, DM scattering in direct detection searches would be one of the very few possible probes of the light-quark Yukawa couplings. The interactions of the Higgs boson with u, d, or s quarks give rise to flavor-conserving neutral currents. Off-shell Higgs contributions in processes with only SM external particles always compete with other, much larger flavor-conserving neutral currents induced by gluon, photon, or Z exchange. This leaves us with two options: either to consider on-shell Higgs decays [13–15], or to use new probes, such as DM scattering in direct detection experiments.

In principle, there is enough information to make a closed argument. Suppose that indirect DM searches yield a positive DM annihilation signal for $m_\chi > m_h/2$. At the end of the high-luminosity LHC run, the Higgs couplings to W, Z, t, and b will be precisely determined. Assuming that DM is a thermal relic interacting only through the Higgs portal, this fixes the value of g_χ since the annihilation cross section for $m_\chi > m_h/2$ is otherwise almost completely controlled by the Higgs couplings to W, Z, and t. In principle, a consistency check that the DM is really interacting through a Higgs portal could be provided, for a very limited range of DM masses $m_\chi \gtrsim m_h/2$, by a 100-TeV hadron collider [10].

After the discovery of DM, the direct detection searches would immediately imply an upper bound on the light-quark Yukawa couplings. As an illustration, consider the excess in γ-ray emmission in the recently discovered dwarf spheroidal galaxy Reticulum 2 [46]. Let's take the bold step of interpreting this signal as originating from DM annihilating into $b\bar{b}$ pairs (see Ref. [114] for details). Assuming the Dirac-fermion DM scenario with purely CP-violating couplings, we obtain a 1σ region in the $m_\chi - \tilde{g}_\chi$ plane that is not yet excluded by direct detection constraints, denoted by the orange lines in Fig. 12. Note that part of this region is consistent with DM furnishing the dominant component of the observed relic density while at the same time not being excluded by the invisible Higgs decay width. Concentrating on the overlap region, $m_\chi \sim 75\,\text{GeV}$, a comparison with the ratios shown in Fig. 11 would immediately imply an upper bound of $\kappa_u \lesssim 10$, $\kappa_d \lesssim 10$, $\kappa_s \lesssim 12$ from the LUX direct detection search (allowing only one of the Yukawa couplings to float at a time).
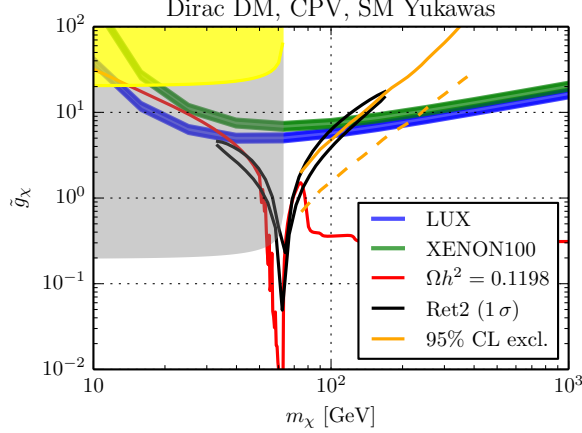
Figure 12: The γ-ray excess in the recently discovered dwarf spheroidal galaxy Reticulum 2, interpreted as a signal of DM annihilating into $b\bar{b}$ pairs, is shown as the black 1σ contour (see Ref. [114] for details). The orange lines show the 95% CL exclusion limits at the 14-TeV LHC (solid line) and a prospective 100-TeV hadron collider (dashed line), obtained by rescaling the bounds given in Ref. [10]. The remaining color coding is the same as in Fig. 2. See text for more details.

These estimates could potentially be loosened by uncertainties in the DM velocity profile and the local DM density. On the other hand, if DM is discovered in direct detection the relative size of the light-quark Yukawas could be probed by comparing scattering rates on different target materials.

An additional cross check of our scenario could be provided by searches for DM production at hadron colliders. In Fig. 12 we denote the 95% CL exclusion limits, assuming 3000/fb of data, at the 14-TeV LHC by a solid orange line and at a prospective 100-TeV hadron collider by a dashed orange line. These curves have been obtained by converting the bounds in Ref. [10] to the case of Dirac DM using `FeynRules` [115] and `MadGraph5` [116]. We see that, while the LHC will be sensitive to a part of the interesting region in parameter space, the scenario of $m_\chi = 75\,\text{GeV}$ DM can be excluded only at a 100-TeV collider.

V. CONCLUSIONS

Not much is known experimentally about the couplings of the Higgs to light quarks. It is entirely possible that the Higgs couples only to the third generation of fermions. Experimen-

tally equally viable is the possibility that the light-quark Yukawas are significantly enhanced, up to $\mathcal{O}(50)$ for κ_s and up to $\mathcal{O}(10^3)$ for κ_u and κ_d. Such extremely large enhancements are not natural from a model-building point of view as they require a large fine tuning of the light-quark masses, but at present cannot be excluded experimentally.

Modified Yukawa couplings to light quarks could have implications for DM searches. In this paper we focused on Higgs-portal DM. We considered constraints on scalar, vector, and fermionic Higgs-portal models of DM from relic density, direct and indirect detection, and the invisible Higgs width. A central result of our analysis is that, for phenomenologically viable Higgs-portal DM, there is a relatively small change in the predictions between the case where the Higgs is SM like and the case where the Higgs couples only to the third generation of fermions. For direct detection this is a consequence of the fact that, for very small light-quark Yukawas, the scattering cross section is dominated by the effective Higgs-gluon coupling, which is obtained by integrating out the heavy quarks. For instance, setting all the light quark Yukawa couplings to zero reduces the direct detection scattering cross section by $\sim 50\%$ compared to the case where the light quark Yukawa couplings are assumed to have SM values. Similarly, the relic abundance and indirect detection signals are dominated by the heaviest kinematically open annihilation channels, diminishing the importance of Higgs couplings to light quarks.

On the other hand, saturating the experimentally allowed values for the light-quark Yukawas, the DM direct detection rates can increase by four orders of magnitude compared to the case where the light-quark Yukawa couplings are kept at their SM values. Moreover, negative values of the light-quark Yukawa couplings can result in a strong reduction of the nucleon scattering rates. The changes in DM annihilation rates are much smaller. The annihilation of DM into light quarks is a subleading effect, unless $m_\chi < m_W$. Even in this case, the dominant annihilation channel is into $b\bar{b}$ pairs, while the annihilation to light quarks can constitute at most an $\mathcal{O}(1)$ fraction if the current experimental upper bounds on the light-quark Yukawa couplings are saturated. A Higgs-portal for DM in this mass range is excluded either by bounds on the invisible Higgs decay width or by indirect DM searches.

We also investigated the expected sizes of corrections to DM phenomenology due to changes in Yukawa couplings in a number of new physics models. The largest deviation in expected DM scattering rate on nucleons was found for a modified Giudice-Lebedev model of light-quark masses where up to an order of magnitude enhancement due to corrections

to light-quark Yukawa couplings are possible. Similarly, an $\mathcal{O}(1)$ change of the scattering rate is anticipated in a pseudo-Goldstone Higgs scenario with composite right-handed light quarks while in RS models with anarchic flavor a reduction of about 20% can be expected. The effects in MFV models, multi-Higgs models with natural flavor conservation, and the type-II two-Higgs-doublet model (i.e., the tree-level Higgs sector of the MSSM), on the other hand, are expected to be much smaller.

Finally, we point out that a discovery of Higgs-portal DM in indirect searches would immediately imply an upper bound on the light-quark Yukawa couplings due to the upper bounds in direct DM searches.

---

[1] B. Patt and F. Wilczek (2006), e-print:hep-ph/0605188.

[2] J. March-Russell, S. M. West, D. Cumberbatch, and D. Hooper, JHEP **0807**, 058 (2008), e-print:0801.3440.

[3] S. Andreas, T. Hambye, and M. H. Tytgat, JCAP **0810**, 034 (2008), e-print:0808.0255.

[4] C. Englert, T. Plehn, D. Zerwas, and P. M. Zerwas, Phys.Lett. **B703**, 298 (2011), e-print:1106.3097.

[5] O. Lebedev, H. M. Lee, and Y. Mambrini, Phys.Lett. **B707**, 570 (2012), e-print:1111.4482.

[6] L. Lopez-Honorez, T. Schwetz, and J. Zupan, Phys.Lett. **B716**, 179 (2012), e-print:1203.2064.

[7] A. Djouadi, A. Falkowski, Y. Mambrini, and J. Quevillon, Eur.Phys.J. **C73**, 2455 (2013), e-print:1205.3169.

[8] A. Greljo, J. Julio, J. F. Kamenik, C. Smith, and J. Zupan, JHEP **1311**, 190 (2013), e-print:1309.3561.

[9] M. A. Fedderke, J.-Y. Chen, E. W. Kolb, and L.-T. Wang, JHEP **1408**, 122 (2014), e-print:1404.2283.

[10] N. Craig, H. K. Lou, M. McCullough, and A. Thalapillil (2014), e-print:1412.0258.

[11] Tech. Rep. ATLAS-CONF-2013-034, CERN, Geneva (2013).

[12] Tech. Rep. CMS-PAS-HIG-13-005, CERN, Geneva (2013).

[13] A. L. Kagan, G. Perez, F. Petriello, Y. Soreq, S. Stoynev, et al. (2014), e-print:1406.1722.

[14] G. Perez, Y. Soreq, E. Stamou, and K. Tobioka (2015), e-print:1503.00290.

[15] C. Delaunay, T. Golling, G. Perez, and Y. Soreq, Phys.Rev. **D89**, 033014 (2014), e-print:1310.7029.

[16] A. Efrati, A. Falkowski, and Y. Soreq (2015), e-print:1503.07872.

[17] R. A. Porto and A. Zee, Phys.Lett. **B666**, 491 (2008), e-print:0712.0448.

[18] J. Kile and A. Soni, Phys.Rev. **D84**, 035016 (2011), e-print:1104.5239.

[19] P. Agrawal, S. Blanchet, Z. Chacko, and C. Kilic, Phys.Rev. **D86**, 055002 (2012), e-print:1109.3516.

[20] I. Masina, P. Panci, and F. Sannino, JCAP **1212**, 002 (2012), e-print:1205.5918.

[21] L. Lopez-Honorez and L. Merlo, Phys.Lett. **B722**, 135 (2013), e-print:1303.1087.

[22] B. Batell, T. Lin, and L.-T. Wang, JHEP **1401**, 075 (2014), e-print:1309.4462.

[23] P. Agrawal, B. Batell, D. Hooper, and T. Lin, Phys.Rev. **D90**, 063512 (2014), e-print:1404.1373.

[24] P. Agrawal, M. Blanke, and K. Gemmler, JHEP **1410**, 72 (2014), e-print:1405.6709.

[25] A. Hamze, C. Kilic, J. Koeller, C. Trendafilova, and J.-H. Yu, Phys.Rev. **D91**, 035009 (2015), e-print:1410.3030.

[26] J. Kile, A. Kobach, and A. Soni (2014), e-print:1411.1407.

[27] C. Kilic, M. D. Klimek, and J.-H. Yu (2015), e-print:1501.02202.

[28] L. Calibbi, A. Crivellin, and B. Zaldivar (2015), e-print:1501.07268.

[29] P. Agrawal, Z. Chacko, C. Kilic, and C. B. Verhaaren (2015), e-print:1503.03057.

[30] J. F. Kamenik and J. Zupan, Phys.Rev. **D84**, 111502 (2011), e-print:1107.0623.

[31] F. Bishara and J. Zupan, JHEP **1501**, 089 (2015), e-print:1408.3852.

[32] I.-W. Kim and K. M. Zurek, Phys.Rev. **D89**, 035008 (2014), e-print:1310.2617.

[33] R. Harnik, J. Kopp, and J. Zupan, JHEP **1303**, 026 (2013), e-print:1209.1397.

[34] V. Khachatryan et al. (CMS) (2015), e-print:1502.07400.

[35] G. Blankenburg, J. Ellis, and G. Isidori, Phys.Lett. **B712**, 386 (2012), e-print:1202.5704.

[36] A. Goudelis, O. Lebedev, and J.-h. Park, Phys.Lett. **B707**, 369 (2012), e-print:1111.1715.

[37] D. Carmi, A. Falkowski, E. Kuflik, T. Volansky, and J. Zupan, JHEP **1210**, 196 (2012), e-print:1207.1718.

[38] J. Brod, U. Haisch, and J. Zupan, JHEP **1311**, 180 (2013), e-print:1310.1385.

[39] F. Goertz, A. Papaefstathiou, L. L. Yang, and J. Zurita, JHEP **1306**, 016 (2013), e-print:1301.3492.

[40] D. E. Ferreira de Lima, A. Papaefstathiou, and M. Spannowsky, JHEP **1408**, 030 (2014), e-print:1404.7139.

[41] K. Olive et al. (Particle Data Group), Chin.Phys. **C38**, 090001 (2014).

[42] S. Chatrchyan et al. (CMS Collaboration), Eur.Phys.J. **C74**, 2980 (2014), e-print:1404.1344.

[43] G. Aad et al. (ATLAS Collaboration), Phys.Rev.Lett. **112**, 201802 (2014), e-print:1402.3244.

[44] M. Endo and Y. Takaesu, Phys.Lett. **B743**, 228 (2015), e-print:1407.6882.

[45] M. Ackermann et al. (Fermi-LAT) (2015), e-print:1503.02641.

[46] A. Drlica-Wagner et al. (Fermi-LAT, DES), Astrophys.J. (2015), e-print:1503.02632.

[47] M. Ackermann et al. (Fermi-LAT) (2015), e-print:1501.05464.

[48] M. Cirelli, G. Corcella, A. Hektor, G. Hutsi, M. Kadastik, et al., JCAP **1103**, 051 (2011), e-print:1012.4515.

[49] G. Jungman, M. Kamionkowski, and K. Griest, Phys.Rept. **267**, 195 (1996), e-print:hep-ph/9506380.

[50] M. A. Shifman, A. Vainshtein, and V. I. Zakharov, Phys.Lett. **B78**, 443 (1978).

[51] D. Akerib et al. (LUX Collaboration), Phys.Rev.Lett. **112**, 091303 (2014), e-print:1310.8214.

[52] E. Aprile et al. (XENON100 Collaboration), Phys.Rev.Lett. **109**, 181301 (2012), e-print:1207.5988.

[53] P. Junnarkar and A. Walker-Loud, Phys.Rev. **D87**, 114510 (2013), e-print:1301.1114.

[54] J. Alarcon, J. Martin Camalich, and J. Oller, Phys.Rev. **D85**, 051503 (2012), e-print:1110.3797.

[55] L. Alvarez-Ruso, T. Ledwig, J. Martin Camalich, and M. Vicente Vacas, EPJ Web Conf. **73**, 04015 (2014).

[56] A. Crivellin, M. Hoferichter, and M. Procura, Phys.Rev. **D89**, 054021 (2014), e-print:1312.4951.

[57] A. Crivellin, F. D'Eramo, and M. Procura, Phys.Rev.Lett. **112**, 191304 (2014), e-print:1402.1173.

[58] A. L. Fitzpatrick, W. Haxton, E. Katz, N. Lubbers, and Y. Xu, JCAP **1302**, 004 (2013), e-print:1203.3542.

[59] S. L. Glashow and S. Weinberg, Phys.Rev. **D15**, 1958 (1977).

[60] E. Paschos, Phys.Rev. **D15**, 1966 (1977).

[61] G. F. Giudice and O. Lebedev, Phys.Lett. **B665**, 79 (2008), e-print:0804.1753.

[62] G. D'Ambrosio, G. Giudice, G. Isidori, and A. Strumia, Nucl.Phys. **B645**, 155 (2002), e-print:hep-ph/0207036.

[63] L. Randall and R. Sundrum, Phys.Rev.Lett. **83**, 3370 (1999), e-print:hep-ph/9905221.

[64] M. J. Dugan, H. Georgi, and D. B. Kaplan, Nucl.Phys. **B254**, 299 (1985).

[65] H. Georgi, D. B. Kaplan, and P. Galison, Phys.Lett. **B143**, 152 (1984).

[66] D. B. Kaplan, H. Georgi, and S. Dimopoulos, Phys.Lett. **B136**, 187 (1984).

[67] D. B. Kaplan and H. Georgi, Phys.Lett. **B136**, 183 (1984).

[68] A. Dery, A. Efrati, Y. Nir, Y. Soreq, and V. Susi, Phys.Rev. **D90**, 115022 (2014), e-print:1408.1371.

[69] A. Dery, A. Efrati, G. Hiller, Y. Hochberg, and Y. Nir, JHEP **1308**, 006 (2013), e-print:1304.6727.

[70] A. Dery, A. Efrati, Y. Hochberg, and Y. Nir, JHEP **1305**, 039 (2013), e-print:1302.3229.

[71] S. El Hedri, P. J. Fox, and J. G. Wacker (2013), e-print:1311.6488.

[72] F. Goertz, Phys.Rev.Lett. **113**, 261803 (2014), e-print:1406.0102.

[73] R. S. Chivukula and H. Georgi, Phys.Lett. **B188**, 99 (1987).

[74] E. Gabrielli and G. Giudice, Nucl.Phys. **B433**, 3 (1995), e-print:hep-lat/9407029.

[75] A. Ali and D. London, Eur.Phys.J. **C9**, 687 (1999), e-print:hep-ph/9903535.

[76] A. Buras, P. Gambino, M. Gorbahn, S. Jager, and L. Silvestrini, Phys.Lett. **B500**, 161 (2001), e-print:hep-ph/0007085.

[77] A. J. Buras, Acta Phys.Polon. **B34**, 5615 (2003), e-print:hep-ph/0310208.

[78] A. L. Kagan, G. Perez, T. Volansky, and J. Zupan, Phys.Rev. **D80**, 076002 (2009), e-print:0903.1794.

[79] J. Aguilar-Saavedra, Nucl.Phys. **B821**, 215 (2009), e-print:0904.2387.

[80] 1244669 (2013), e-print:1307.7135.

[81] 1245017 (2013), e-print:1307.7292.

[82] A. Falkowski, C. Gross, and O. Lebedev (2015), e-print:1502.01361.

[83] V. Martin-Lozano, J. M. Moreno, and C. B. Park (2015), e-print:1501.03799.

[84] H. E. Haber and G. L. Kane, Phys.Rept. **117**, 75 (1985).

[85] A. Falkowski, F. Riva, and A. Urbano, JHEP **1311**, 111 (2013), e-print:1303.1812.

[86] B. Grinstein and P. Uttayarat, JHEP **1306**, 094 (2013), e-print:1304.0028.

[87] T. Gherghetta and A. Pomarol, Nucl.Phys. **B586**, 141 (2000), e-print:hep-ph/0003129.

[88] Y. Grossman and M. Neubert, Phys.Lett. **B474**, 361 (2000), e-print:hep-ph/9912408.

[89] S. J. Huber and Q. Shafi, Phys.Lett. **B498**, 256 (2001), e-print:hep-ph/0010195.

[90] S. J. Huber, Nucl.Phys. **B666**, 269 (2003), e-print:hep-ph/0303183.

[91] A. Azatov, M. Toharia, and L. Zhu, Phys.Rev. **D80**, 035016 (2009), e-print:0906.1990.

[92] S. Casagrande, F. Goertz, U. Haisch, M. Neubert, and T. Pfoh, JHEP **0810**, 094 (2008), e-print:0807.4937.

[93] M. Bauer, S. Casagrande, U. Haisch, and M. Neubert, JHEP **1009**, 017 (2010), e-print:0912.1625.

[94] R. Malm, M. Neubert, K. Novotny, and C. Schmell, JHEP **1401**, 173 (2014), e-print:1303.5702.

[95] P. R. Archer, M. Carena, A. Carmona, and M. Neubert, JHEP **1501**, 060 (2015), e-print:1408.5406.

[96] M. Blanke, A. J. Buras, B. Duling, S. Gori, and A. Weiler, JHEP **0903**, 001 (2009), e-print:0809.1073.

[97] M. Blanke, A. J. Buras, B. Duling, K. Gemmler, and S. Gori, JHEP **0903**, 108 (2009), e-print:0812.3803.

[98] M. E. Albrecht, M. Blanke, A. J. Buras, B. Duling, and K. Gemmler, JHEP **0909**, 064 (2009), e-print:0903.2415.

[99] K. Agashe, G. Perez, and A. Soni, Phys.Rev. **D75**, 015002 (2007), e-print:hep-ph/0606293.

[100] K. Agashe, A. Azatov, Y. Cui, L. Randall, and M. Son (2014), e-print:1412.6468.

[101] B. M. Dillon and S. J. Huber (2014), e-print:1410.7345.

[102] G. Cacciapaglia, C. Csaki, J. Galloway, G. Marandella, J. Terning, et al., JHEP **0804**, 006

(2008), e-print:0709.1714.

[103] K. Agashe, G. Perez, and A. Soni, Phys.Rev. **D71**, 016002 (2005), e-print:hep-ph/0408134.

[104] K. Agashe, G. Perez, and A. Soni, Phys.Rev.Lett. **93**, 201804 (2004), e-print:hep-ph/0406101.

[105] Tech. Rep. ATLAS-CONF-2015-009, CERN, Geneva (2015).

[106] D. B. Kaplan, Nucl.Phys. **B365**, 259 (1991).

[107] K. Agashe and R. Contino, Phys.Rev. **D80**, 075016 (2009), e-print:0906.1542.

[108] M. Gillioz, R. Grober, C. Grojean, M. Muhlleitner, and E. Salvioni, JHEP **1210**, 004 (2012), e-print:1206.7120.

[109] C. Delaunay, C. Grojean, and G. Perez, JHEP **1309**, 090 (2013), e-print:1303.5701.

[110] A. Pomarol and F. Riva, JHEP **1208**, 135 (2012), e-print:1205.6434.

[111] A. Azatov, G. Panico, G. Perez, and Y. Soreq, JHEP **1412**, 082 (2014), e-print:1408.4525.

[112] M. Redi and A. Weiler, JHEP **1111**, 108 (2011), e-print:1106.6357.

[113] M. Redi, Eur.Phys.J. **C72**, 2030 (2012), e-print:1203.4220.

[114] A. Geringer-Sameth, M. G. Walker, S. M. Koushiappas, S. E. Koposov, V. Belokurov, et al. (2015), e-print:1503.02320.

[115] A. Alloul, N. D. Christensen, C. Degrande, C. Duhr, and B. Fuks, Comput.Phys.Commun. **185**, 2250 (2014), e-print:1310.1921.

[116] J. Alwall, R. Frederix, S. Frixione, V. Hirschi, F. Maltoni, et al., JHEP **1407**, 079 (2014), e-print:1405.0301.